Investigation of Concentrating Parabolic Collectors Integrated with Hot Water Cylinder for Solar Water and Space Heating Applications

Hooman Azad Gilani

Submitted to the
Institute of Graduate Studies and Research
in partial fulfillment of the requirements for the degree of

Master of Science
in
Mechanical Engineering

Eastern Mediterranean University
January 2019
Gazimağusa, North Cyprus

Approval of the Institute of Graduate Studies and Research

Assoc. Prof. Dr. Ali Hakan Ulusoy
Acting Director

I certify that this thesis satisfies all the requirements as a thesis for the degree of Master of Science in Mechanical Engineering.

Assoc. Prof. Dr. Hasan Hacisevki
Chair, Department of Mechanical Engineering

We certify that we have read this thesis and that in our opinion it is fully adequate in scope and quality as a thesis for the degree of Master of Science in Mechanical Engineering.

Asst. Prof. Dr. Devrim Aydin
Supervisor

Examining Committee

1. Assoc. Prof. Dr. Hasan Hacisevki

2. Asst. Prof. Dr. Devrim Aydin

3. Asst. Prof. Dr. Huseyin Camur

ABSTRACT

Flat plate collectors are the most common type of collectors used in residential applications. However, efficiency of these collectors decrease in situations when the available beam radiation is limited.

This study aims to investigate the potential of Compound Parabolic Collectors (CPC) for being utilized in residential solar water heating systems, instead of conventional flat plate collectors. To do so, several related parameters like useful solar heat gains, auxiliary power requirements and efficiencies of both collector types under same operating conditions are examined and compared.

Within the study, a solar water heating system consisting of a solar collector, a storage tank and a circulating pump was simulated in TRNSYS. The simulations were carried out in the first week of January for two different cities, Nicosia with abundant and London with limited solar radiations. Water circulates between the collector and the tank to generate solar sourced heat and to store it for later use. Tank temperature is maintained at 60^{o}C thought the simulation. An electric heater is considered as auxiliary heating device to boost the water temperature to the set point when there is not sufficient solar radiation available. The results show that in both considered locations (Nicosia and London) CPC provides higher outlet temperatures compared to flat plate collector. The gap is more meaningful particularly in days with low beam radiation. According to the results, weekly efficiency of CPC and flat plate collector are 34% and 21% for Nicosia and 30% and 15% for London, respectively.

In addition, useful solar energy gain of CPC is 61% and 97% more than that of the flat plate collector in Nicosia and London, respectively. As a result, auxiliary power requirements are 11% and 6% less for CPC, respectively. Also, CPC provides a higher yearly performance in both cities.

Keywords: Solar Energy, Water Heating, TRNSYS, Compound Parabolic Collector, Flat Plate Collector

ÖZ

Düz plakalı kollektörler güneş enerjili sıcak su eldesi amacıyla binalarda yaygın olarak kullanılmaktadır. Ancak bu tür güneş kollektörü sistemlerinin verimi, güneş ışınımı miktarının sınırlı olduğu koşullarda düşüktür.

Bu çalışma, binalarda güneş enerjili sıcak su üretimi uygulamalarında düz plakalı güneş kollektörleri yerine yoğunlaştırmalı parabolik güneş kollektörlerinin kullanılmasının uygunluğunu karşılaştırmalı olarak incelemektedir. Bu bağlamda, aynı çalışma koşulları altında, düz plakalı ve yoğunlaştırmalı parabolik güneş kollektörlerinin yararlı güneş enerjisi kazancı, ilave enerji gereksinimleri ve verimlilik değerleri karşılaştırmalı olarak analiz edilmiştir.

Çalışma kapsamında, güneş kollektörü, sıcak su depolama tankı ve sirkülasyon pompasından meydana gelen sistem TRNSYS programında simüle edilmiştir. Simülasyonlar ocak ayı ilk haftası için, yüksek ve düşük güneş ışınımı değerlerine sahip Lefkoşa ve Londra şehirlerine uygulanmıştır. Sistemde su, güneş kollektörleri ve su tankı arasında sirküle edilerek, daha sonra kullanılmak üzere sıcak su eldesi sağlanmaktadır. Simulasyonlar sırasında su sıcaklığı ayar derecesi 60 °C olarak seçilmiştir. Güneş ışınım değerinin yeterli olmadığı durumda su sıcaklığını ayar noktasında tutabilmek için sistemde elektrikli su ısıtıcı ünitesi kullanılmıştır.

Çalışma sonuçlarına göre seçilen her iki konumda da (Lefkoşa ve Londra) yoğunlaştırmalı parabolik güneş kollektörü, düz plakalı güneş kollektörüne göre daha yüksek çıkış suyu sıcaklığı sağlamaktadır. Bunun yanında yoğunlaştırmalı parabolik ve düz plakalı kollektör performansı arasındaki fark, güneş ışınımı değerinin düşük

olduğu günlerde daha yüksek olmaktadır. Simulasyon sonuçlarına göre, ocak ayı ilk haftasında yoğunlaştırmalı parabolik ve düz plakalı kollektör ortalama verimleri Lefkoşa için 34% ve 21%, Londra için ise 30% ve 15% olarak bulunmuştur.

Ayrıca, Lefkoşa ve Londra koşulları için, yoğunlaştırmalı parabolik güneş kollektörü yararlı güneş enerjisi kazancı, düz plakalı kollektöre göre sırasıyla 61% ve 97% daha yüksek bulunmuştur. Bunun sonucu olarak, Lefkoşa ve Londra koşullarında, ilave elektrik enerjisi gereksinimi, younlaştırmalı parabolik kollektrörler için 11% ve 6% daha düşük olarak hesaplanmıştır. Bunun yanında uzun dönemli çalışma koşullarında da yoğunlaştırmalı güneş kollektörü yıllık ortalama performansının düz plakalı güneş kollektörlerine göre daha yüksek olduğu belirlenmiştir.

Keywords: Güneş Enerjisi, Su Isıtma, TRNSYS, Yoğunlaştırmalı Parabolik Kollektör, Düz Plakalı Kollektör

To

My Beloved Parents

ACKNOWLEDGMENT

First of all, I must express my very profound gratitude to my family, especially my parents, for being lighting candles for me through every wind and rain, for providing me with unfailing support and continuous encouragement whenever I needed.

I also would like to thank my thesis advisor Assist. Prof. Dr. Devrim Aydin for his unlimited support. Dr. Aydin was available anytime during night time or holidays whenever I ran into a trouble or had a question about my research or writing. He always encouraged and motivated me and his interesting and innovative ideas gave me prospective of what could be done to improve the research. Working with Dr. Aydin was a pleasant experience for me.

Also, I should thank Prof. Dr. Ugur Atikol for always sharing his research experiences with me generously and also referring me to the thesis of his former master student Sarvenaz Sobhansarbandi regarding simulation of CPCs with TRNSYS. Many thanks to Assist. Prof. Dr Murat Ozdenefe for offering solar energy course in our department. This course provided me with a very good foundation in solar energy fundamentals so I could pursue more in depth detailed studies in the area.

I hope this thesis could be useful for future students to give them some useful information about solar thermal processes, flat plate collectors, CPCs, related mathematical formulations and simulation with TRNSYS.

TABLE OF CONTENTS

LIST OF TABLES

LIST OF FIGURES

LIST OF SYMBOLS

A_a	[m^2]	Aperture area
A_c	[m^2]	Collector area
A_{ref}	[m^2]	Reflector area
a_0	[-]	Collector intercept efficiency
a_1	[W/m^2-K]	Collector efficiency slope
a_2	[W/m^2-K^2]	Collector efficiency curvature
b_0	[-]	1st-order incidence angle modifier
b_1	[-]	2nd-order incidence angle modifier
C	[-]	Concentration ratio
C_p	[J/kg-K]	Specific heat
F_b	[-]	Control function
F_{gnd}	[-]	View factor to the ground
F_R	[-]	Collector heat removal factor
F_{sky}	[-]	View factor to the sky
F'	[-]	Collector efficiency factor
I	[W/m^2]	Rate of total solar radiation on a horizontal surface
I_{bT}	[W/m^2]	Rate of solar beam radiation on a tilted surface
I_d	[W/m^2]	Rate of solar diffuse radiation on a horizontal surface
I_T	[W/m^2]	Rate of radiation entering the reflector aperture
K	[m^{-1}]	Extinction coefficient

$K_{\tau\alpha}$	[-]	Incidence angle modifier
L	[m]	Cover thickness
$\dot{L}_s$	[W]	Rate of thermal energy to the load
m	[kg]	Mass
$\dot{m}$	[kg/s]	Mass flow rate
$(mC_p)_s$	[J/K]	Product of the mass and the specific heat of the tank's medium
n_g	[-]	Refractive index
n_r	[-]	Average number of reflections
$\dot{Q}_u$	[W]	Rate of useful solar energy gain of a collector
r	[-]	Correction ratio
$r_\perp$	[-]	Perpendicular component of reflection of unpolarized radiation
$r_\parallel$	[-]	Parallel component of reflection of unpolarized radiation
S	[W/m^2-K]	Rate of absorbed solar energy
T_a	[^{o}C]	Ambient temperature
$T_a^{'}$	[^{o}C]	Storage tank surrounding temperature
T_i	[^{o}C]	Collector inlet temperature
T_o	[^{o}C]	Collector outlet temperature
T_s	[^{o}C]	Storage tank temperature
T_s^+	[^{o}C]	Storage tank temperature after one hour
(TA)	[-]	Overall transmittance-absorbtance product
t	[s]	Time
$\triangle t$	[s]	Time interval (one hour)

U_L	[W/m^2-K]	Collector overall heat loss coefficient
$U_{L/T}$	[W/m^2-K^2]	heat loss coefficient dependency on temperature
$(UA)_s$	[W/K]	Product of the storage tank heat loss coefficient and area
α	[-]	Short-wave absorptance of the absorber plate
α_{eff}	[-]	effective abrobtance
β	[^{o}]	Collector tilt angle
γ	[^{o}]	Surface azimuth angle
γ_s	[^{o}]	Solar azimuth angle
η	[-]	Collector efficiency
θ	[^{o}]	Incident angle for beam radiation
θ_1	[^{o}]	Angle of incidence
θ_2	[^{o}]	Angle of refraction
θ_c	[^{o}]	Half-acceptance angle
θ_d	[^{o}]	Diffuse effective incidence angle
θ_g	[^{o}]	Ground reflected effective incidence angle
θ_l	[^{o}]	Longitudinal acceptance angle
θ_t	[^{o}]	Transverse acceptance angle
θ_z	[^{o}]	Zenith angle
ρ_{eff}	[-]	Reflectance of the cover for diffuse radiation
ρ_d	[-]	Effective reflectance of the reflector
ρ_g	[-]	Ground reflectance
ρ_R	[-]	Reflectivity of the CPC walls

$\rho_{\perp}$	[-]	Reflectance perpendicular component of polarization
$\rho_{\parallel}$	[-]	Reflectance parallel component of polarization
τ	[-]	Transmittance of cover
τ_a	[-]	Transmittance with only absorption losses have been considered
$\tau_{\perp}$	[-]	Transmittance perpendicular component of polarization
$\tau_{\parallel}$	[-]	Transmittance parallel component of polarization
$(\tau\alpha)$	[-]	Product of the cover transmittance and the absorber absorptance
$(\tau\alpha)_b$	[-]	$(\tau\alpha)$ for beam radiation (depends on the incidence angle θ)
$(\tau\alpha)_d$	[-]	$(\tau\alpha)$ for sky diffuse radiation
$(\tau\alpha)_g$	[-]	$(\tau\alpha)$ for grand reflected radiation
$(\tau\alpha)_n$	[-]	$(\tau\alpha)$ at normal incidence

Chapter 1

INTRODUCTION

Estimates show that the proven oil sources could only nurture our civilization increasing energy demand rates by less than 50 years. This is based on the assumption that the worldwide energy consumption rate remains at its present amount during upcoming decades. Although reserves for coal can supply our energy demand for a much longer time period, the environmental pollution caused by this energy source prevent it from becoming a reliable alternative for oil, even in mid-term period.

As a result of decrease in oil resources, their prices accelerate more quickly so that other alternative energy source like renewable energies are becoming more economical. Several various forms of alternative energy sources are available which could be used instead of fossil fuels. Solar energy as a sustainable source of energy is very promising. Annual solar energy potential available on earth is more than enough to meet all energy demand on the planet. Many high-tech and also developing countries are investing hugely on solar energy for both electric and thermal power generation.

1.1 The Significance of the Study

Solar water heating systems for either heating or domestic hot water applications have been commercialized and are widely used in several countries in the world.

In Northern Cyprus fossil fuels are imported and are consumed in conventional power generation plants to generate electricity. Consequently, electricity is very costly. As a result, solar energy is widely used to supply heat for domestic hot water so that a flat plate collector for heating water is an essential component of almost every building. Conventional flat plate collectors are the most common solution in residential domestic hot water applications in Northern Cyprus. High efficiency, affordability, easy installment and maintenance are among the reasons for popularity of flat plate collectors. Increasing the efficiency of the solar collector, which is the heart of a solar water heating system, would result in reduction of auxiliary energy requirement. This, especially in a long term, would benefit the end user financially and the society economically and environmentally, because less overall eclectic power consumption means less fossil fuel combustion and so less harmful gas emissions. Thus, even a small increase in the efficiency of solar collectors could result in a significant reduction of fusil fuel consumption rates.

Many advances have been achieved in designing and manufacturing flat plate collectors and highly efficient flat plate collectors are available in the market. However, these types of collectors have some major shortcomings. Most importantly, during winter time, which sun's rays fall at a low angle, available heat gain of flat plate collectors drops significantly and more auxiliary power supply would be required. In order to overcome this flaw and other limitations, more advanced solar collectors are needed to be designed. One of the potential designs to increase the efficiency of solar collectors is using the concentration concept. In concentrating solar collectors, sun radiation is reflected by a relatively large reflector area to a smaller receiver area. Employing concentrating solar collectors usually requires implementation of a

tracking system, since collector should be oriented exactly in a way that it reflects the incoming rays to the receiver area. Complexity and cost of tracking systems limit the application of concentrating collectors to power generation and industrial applications.

Compound Parabolic Collectors (CPCs) are one of the promising concentrating solar collectors for domestic hot water applications, since they can produce high temperature water even when sun rays don't strike the collector at an optimized angle, meaning they can be implemented without a tracking system. Since the angle of the sun on the collector surface continually varies as earth moves, most of the sun's rays strike the collector surface at an angle. This is very important in transitional period (spring/autumn), when up to 80% of the sun's rays fall at a low incident angle. Therefore, using CPCs can improve the useful heat gain from solar radiation even with a weak sunlight at a low angle of incidence.

This type of solar collector usually is employed in industrial and medium temperature applications. In this study, the performance of a CPC in a low temperature solar heating water system will be investigated.

1.2 Objectives

In this study, the aim is to numerically compare the performance of two types of solar collectors in residential solar water heating systems, one is a typical flat plate collector and the another one is a CPC collector. The design and dimensions of the CPC will be considered in a way that makes it practically possible to employ the CPC in a domestic solar water heating system, without any tracking system requirement.

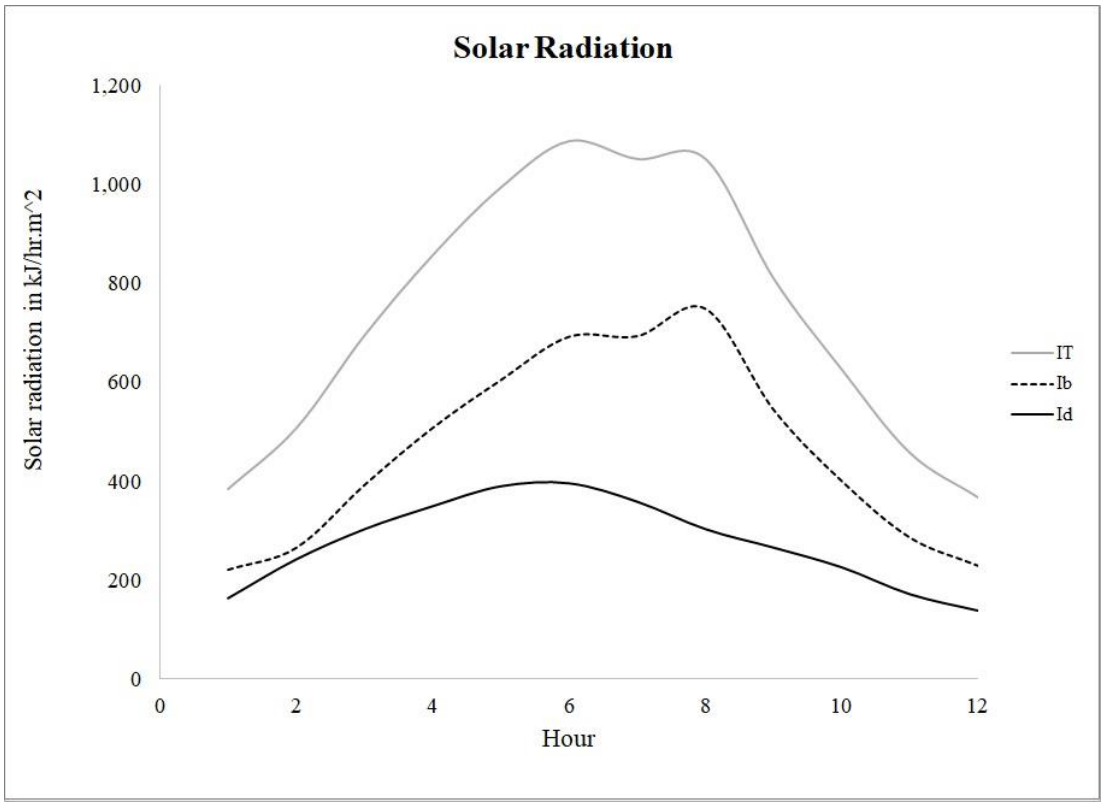

(a)

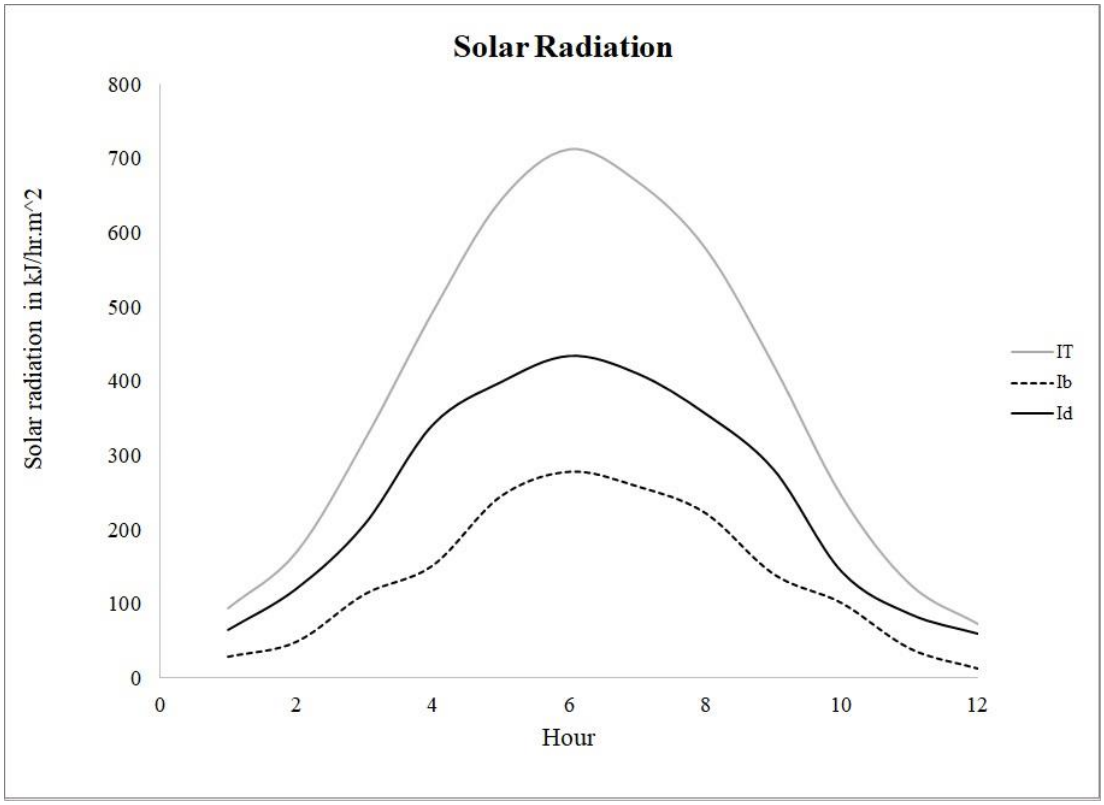

(b)

Figure 1: Yearly Global, Beam and Diffuse Radiation (a for Nicosia (b for London

The system will be integrated with a hot water storage tank which the heated water from the collector would be directed to the storage tank in order to be stored or used. The weekly efficiency of both collectors will be evaluated numerically and will be compared. Also weekly auxiliary power requirement of two collectors will be determined and compared to evaluate how much energy could be saved if a CPC is utilized instead of a flat plate collector.

Moreover, the study will be carried out in two different cities with different climate and weather conditions, one Nicosia with abundant solar radiation and the other, London, a well-known example of a cloudy rainy city. Yearly global, beam and diffuse radiations of Nicosia and London are shown in Figure 1. As it is shown, a lot more beam radiation is available in Nicosia, compared with London. So, running the simulation for this two cities, one with abundant total and beam radiations and the other with limited radiation, will provide a better understanding of how a CPC's performance is, compared to that of a flat plate collector, in different climates.

1.3 Limitations of the Study

The accuracy and exactness of any simulation depends on the two main factors. One is the mathematical model that is used to describe the system or the phenomena, and the other is the skill with which they are used. Decades of experience with simulations and validations, has resulted in reliable simulation tools. Yet, no mathematical model or simulation tool can represent in detail all of the phenomena occurring in a system. Possibilities like leaks, failure of controllers, poor installation and etc. usually are not considered in simulations. Or as an another instance, thermal capacity of a collector might be neglected in calculations, while in real experience, it could affect the temperature variations of the fluid sensibly.

Enough experience and skill in performing a simulation is another critical issue. It's obvious that the result of any simulation is strongly depends on the assumptions made and the parameters used in the process. Making a very exact comparison between two different collector types requires choosing exactly identical thermal and optical parameters for both collectors such as collector overall heat loss coefficient, cover transmittance, absorptance of absorber plate and etc. However, this is not the case in this study, because in this study parameters of both collector types have been extracted from valid references. Nevertheless, they don't necessarily have identical properties. A standard quadratic efficiency equation is available for most commercial flat plate collectors which is the basis of analyzing these collectors in the present study. Nevertheless, such a standard equation is barely available for CPCs.

In addition, the collector overall heat loss coefficient is usually a function of temperature. Collector efficiency factor is a function of collector overall heat loss coefficient and thus it's also varying with temperature. Yet, for CPC, both these quantities are entered to TRNSYS as constant parameters. This could add some uncertainty to the numerical study.

Despite all these issues, the two collectors have the same areas and fluid mass flow rates and are operated in identical systems. It could be concluded even though there are some limitations in this study, like any other numerical study, still the results provide valuable information about the performance of CPC in domestic hot water applications, which can be a subject for experimental and more extensive studies.

1.4 Organization of the Study

The structure of current study has organized in 6 chapters. Chapter 2 provides a concise, yet detailed and informative, review on energy crisis, importance of alternative energies, solar thermal processes, different solar collector types, and finally, some research and work regarding CPCs. Chapter 3 begins with the solar hot water system and its components.

Next, detailed mathematical description of the system is presented. TRNSYS contains several components for modeling a flat plate collector. In this study a quadratic efficiency flat plate collector, with 2nd order incidence angle modifiers, has been used. Chapter 4 starts with a brief introduction on TRNSYS and brings some discussions regarding advantages and disadvantages of using simulations to study physical systems and phenomena. Then detailed information about the model used to simulate a solar assisted water heating system is provided. All employed components are introduced and described. A table of the parameters used in the simulation also is available.

In chapter 5 results of simulations are reported and compared. Different graphs show collector outlet temperature, efficiency, useful heat gain, auxiliary power, tank temperature and other several quantities for both collectors and cities, for the first week of January. Also weekly amounts of useful solar energy gain, required auxiliary energy, collector efficiency and percentage of auxiliary energy reduction are calculated and listed for all cases.

Finally, in chapter 6 conclusion is brought up. This final chapter concludes that using a CPC in a domestic solar hot water system can reduce the weekly auxiliary power requirement meaningfully, compared with the case a typical flat plate collector is used, in both sunny or cloudy climates. This, in turn, means in a long run replacing a flat plate collector with a CPC could decrease the amount of energy purchase, and saves the end user energy cost.

Chapter 2

LITERATURE REVIEW

2.1 Energy Demand and Renewable Energies

Technological and industrial achievements in recent years have boosted energy consumption rates considerably. The rapid global economic and industrial growth and it's consequent accelerating demand for energy, has made energy issue one of the main challenges in our time. Sustainable development and welfare is not possible without adequate energy sources available.

In Figure 2 the growth in the world energy's demand from 1970 to 2010 is illustrated [1]. The last tree columns are the projected values for the tree up coming decades. It shows that the world energy consumption over last 50 years has almost tripled. Total world energy demand would grow by approximately a third by 2040 which is a much slower rate compared with the growth rate of the previews 25 years. As it is observed, currently, oil and gas are the main energy sources. Discovering increasing amount of oil resources and very low cost production of this energy have been the main reasons for the rapid increase in oil demand across the world. However, it is expected that world demand for fossil fuels will exceed the annual production during almost next two decades [2]. Moreover, at the current rate of consumption, proven oil and gas reserves could be sufficient for world energy demand only for less than 70 years [3].

In addition to accelerated increase in the global demand for energy and limited fusil sources, environmental issues and climate change have become one of the most urgent worldwide problems. Emitting huge amounts of carbon dioxide to the atmosphere, which is one of the products of all combustion processes, is one the main causes of greenhouse and global warming effects which currently threaten all life forms on planet earth. Fossil fuel combustion has a very high contribution to the CO_2 emissions to the atmosphere. World CO_2 emissions from fuel combustion almost has been doubled from 1971 to 2015 [4]. Decreasing CO_2 emissions has become an inevitable issue in economical and industrial considerations.

Diminishing fossil fuel resources and environmental problems have drawn many efforts to find alternative energy sources. Finding and designing energy efficient and environmental friendly devices nowadays is an interest for many advanced and developing countries and is attracting and increasing amount of investment. According to International Energy Agency (IEA), the current increasing energy demand and its continuous trend in the following decades, will make it necessary to make more than $20 trillion new investments in energy industry [5].

Renewable energies such as solar, wind, geothermal, biomass, oceanic and other forms of energy, have drawn a lot of attention in the recent years due to their environmental friendly nature and sustainability. Sustainable development could be defined as a development that ‘meets the needs of the present without compromising the ability of future generations to meet their own needs’ [6].

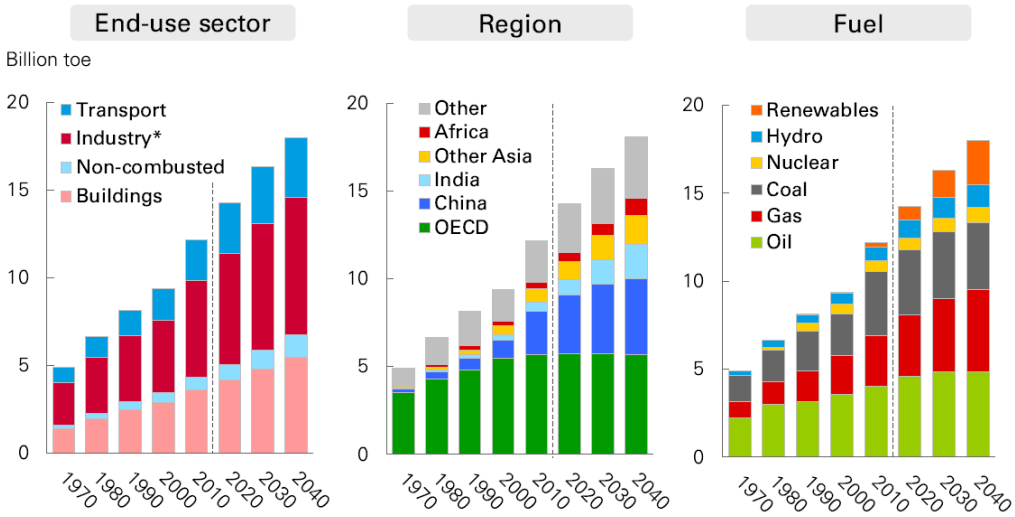

Figure 2: Total World Energy Consumption in Billion Toe [1]

Solar thermal energy is the most abundant source of renewable energy among of all alternative ones. About 0.01% of the total annual solar radiation reaching the earth's surface is sufficient to meet the world's total annual primary energy consumption of 450EJ [2].

There are two main categories of solar energy application. One is solar electrical power applications and the other one is solar thermal applications. The solar electrical power generation is based on the photovoltaic effect which had been discovered by Becquerel in 1839. In photovoltaic conversion, sunlight is converted directly into electricity without introducing any external work [7]. Photovoltaic effect can be described as a process in which electrical voltage is produced when two dissimilar materials, closely contacted to each other, are exposed to sunlight or any other similar radiation. Photovoltaic cells are made of semiconductors, which are the materials that conduct electricity in some conditions and not in other conditions. Silicon (Si) and compounds of cadmium sulphide (Cds) are among the materials most commonly used in photovoltaic cells.

The biggest advantage of photovoltaic cells is their stand-alone system construction. They are widely used in different applications like power source, solar home systems, satellites, communication and a lot more. Due to this wide range of applications, the demand for photovoltaics is growing every year. A review of photovoltaic systems and technologies can be found in Ref. [7].

In recent decades many researches and studies have been conducted on designing and developing innovative solutions in solar electrical power and thermal applications. The rest of this study is concerned with solar thermal applications with focusing on solar water heating applications.

2.2 Solar Thermal Processes

This section briefly reviews the applications that produce thermal energy by harnessing and utilizing solar radiation intensity. Some of these applications are domestic hot water (DHW), space heating, space cooling and refrigeration and Industrial process heat.

2.2.1 Domestic Hot Water

Supplying domestic hot water is the most common application of the solar collectors installed all around the world. In this type of solar application, solar radiation is absorbed by a solar collector and then this radiation is converted into heat. This heat is then transferred to a fluid such as water or an antifreeze such as a glycol-water mixture. In case of using an antifreeze, a heat exchanger is employed to transfer heat from antifreeze to the hot supplying water [6]. Usually hot water is directed to a storage tank.

In passive system heat transfer fluid is transported naturally, while in active systems this is done by forced circulation. A typical circuit of an active solar DHW system with a storage tank and a heat exchanger is shown in Figure 3 [8].

2.2.2 Space Heating

Solar space heating can be used in conjunction with solar DHW system or separately. A conventional heating system like fan coil system or underfloor heating arrangement can be supported by an active solar system. In this case, system configuration again includes heat exchangers, storage thanks and pumps. However, in this case two separate water loops are required, one for heating and one for DHW. Combisystems which are the combination of water and space heating systems are commonly used in Austria, China and some parts of Europe and about 10% to 30% or in some situations more fraction of the total heat demand can be supplied by these combined systems [9]. Space heating also could be achieved by heating the air directly and directing the hot air to the heated space. In this case air heaters are used.

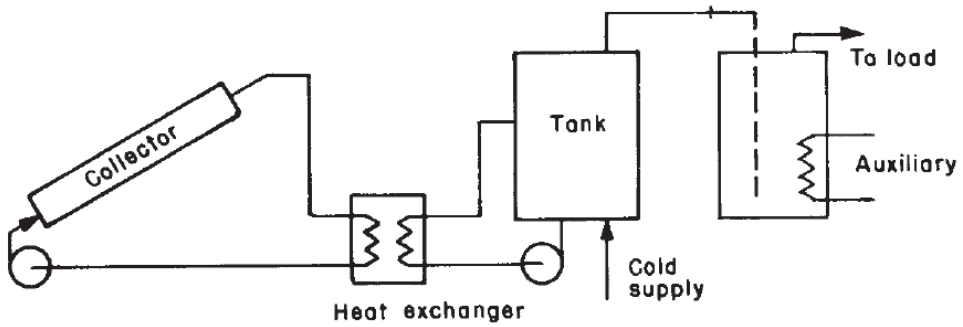

Figure 3: A Typical Active Solar DHW System with a Heat Exchanger Between Collector and Tank [8]

2.2.3 Space Cooling and Refrigeration

There are tree methods for solar cooling: Absorption cycles, adsorption (desiccant) cycles and solar mechanical systems. A schematic of an absorption cycle is shown in Figure 4 [10]. It is consisted of four main components: evaporator, condenser, generator and absorber. Low pressure evaporating refrigerant enters the evaporator, taking the heat from the cooling fluid, and evaporates. The vapor is then absorbed by the absorbent in the absorber. Next, high moisture-content absorbent is directed to the generator in order to separate the absorbent and the refrigerant vapor. Separated refrigerant vapor is condensed in the condenser and returns to the evaporator to complete the cycle. The cooling effect in the evaporator can be used for cooling applications. Details about operation and configuration of an absorption cooling system can be found in Ref. [10]. Absorption and adsorption processes differ by whether or not the desiccant undergoes a chemical change as it absorbs the moisture. Absorption changes the physical structure of the desiccant, while adsorption does not [10]. In the generator, a high temperature heat source is needed which makes absorption cooling systems a suitable design for solar cooling.

It should be mentioned that direct fired absorption systems are widely used in middle east, due to the low cost and availability of fossil fuels in these countries. In this type of absorption systems, heat is supplied to the generator directly by the burner. However, this fossil-fuel consuming absorption system is not environmentally friendly since CO_2 and other harmful combustion products are emitted to the atmosphere as fuel is burned in the burner. Also low efficiency of these systems makes them favorable only if the fuel is available with a very low cost, which is the case in Middle Eastern counties.

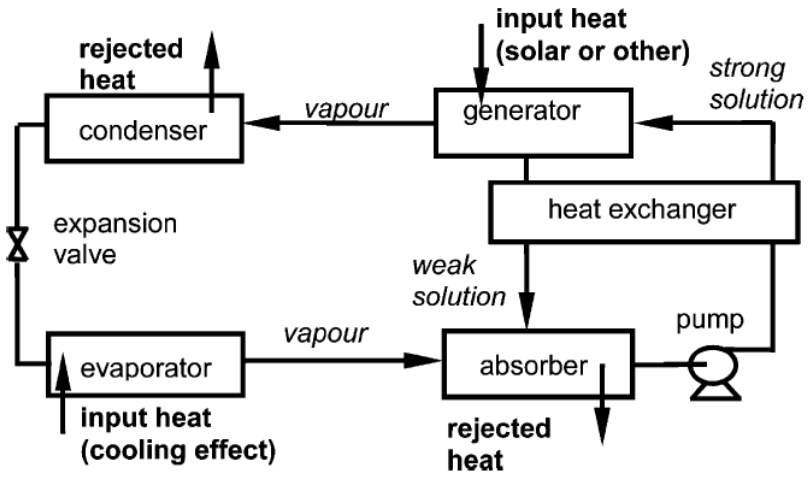

Figure 4: A Schematic of an Absorption Cycle [10]

In solar mechanical systems, a conventional compression refrigeration cycle is driven by a solar-powered prime mover. Two approaches are available. One approach is to utilize photovoltaics to convert solar radiation to electricity and then use this electricity as a power supply for the compression refrigeration cycle. However, low field efficiency of photovoltaics, around 10-15% depending on the type of the cells used [11], makes these systems operate with low overall efficiency. Another alternative is to use a Rankine heat engine as a solar- powered prime mover. In this scheme, heat is delivered from the sun using a solar collector. Then, using the heat engine, this heat is converted to shaft work which consequently drives the compressor in the standard compression refrigeration cycle. Most of the times, when the compressor is coupled with the Rankine heat engine, the power supplied by the heat engine is not matched with the power required by the compressor. So an auxiliary energy must be available in case there is not enough power generated from the heat engine. In case of excess power generation, extra electricity can be either stored or be used for other purposes.

2.2.4 Industrial Process Heat

About 15% of the southern European countries' overall energy demand is consumed in industry [12]. Heat production for industrial processes is another application of solar thermal energy. Some of these applications are sterilising, pasteurizing, drying, distillation, evaporation, washing and cleaning. These are among medium temperature level (80-240^{o}C) thermal processes which, along with medium temperature processes, demand for 300TWh energy supply per year in EU [13]. Ref [14] presents some of the most important processes and the corresponding temperature range for each process. These processes, because of their temperature levels, offer suitable conditions for the application of solar energy.

2.3 Solar Collectors

Solar Collector is the main essential part of every solar water heating system. Solar collectors are used to absorb solar radiation and convert it to useful thermal energy.

This thermal energy is used to heat a working fluid which is usually water, air or oil. The collected solar energy is either directed to a solar application or is stored in a thermal energy storage tank for use at times which there is no sun radiation available. An efficient solar collector is described by its capability to absorb sun's radiation and convert it to heat with minimal optical and thermal losses.

Generally, solar collectors are divided in two main categories: non-concentrating and concentrating collectors. In non-concentrating collectors, solar radiation collection part and solar radiation absorption part have the same area, while in concentrating collectors, collection area is relatively larger than the absorption area.

Non-concentrating collectors are suitable for moderate temperature applications, about 100^{o}C above ambient temperature. These collectors can collect both solar beam and diffuse radiations and so do not require a tracking system [8]. Non-concentrating collectors include flat plate collectors (FPC) and evacuated tube collectors (ETC). More information regarding non-concentrating collectors are available in Ref. [12].

In solar thermal applications with medium temperature range requirement about 80-250^{o}C, concentrating collectors are favorable [15]. Concentrating collectors are usually made up of one or more collection reflectors, absorber receiver, heat exchanger and working fluid. They might use a tracking system or a thermal storage tank as well, depending on the application. There are several types of concentrating collectors with different temperature delivery ranges suitable for different applications. Temperatures up to 900^{o}C are available in special concentrating collectors called solar dishes [16]. Details about construction and application of different concentrating collectors are available in Refs. [12] and [16].

In this study, the focus would be on stationary solar collectors. These collectors are fixed in their positions and don't track the sun. The type of collectors fall in this category are the tree followings:

1-Flat plate collectors (FPC)

2-Stationary compound parabolic collectors (CPC)

3-Evacuated tube collectors (ETC)

In the following sections, each type will be investigated and discussed in more details.

This study is focused on compound parabolic collectors, a concentrating collector type which are favorable for medium temperature applications with a maximum temperature output of 250^{o}C [16].

2.3.1 Flat Plate Collectors

Flat plate collectors (FPC) are the most common collectors in solar water heating systems. They can deliver hot water to approximately 100^{o}C above ambient temperature [8]. Since flat plate collectors could collect both beam and diffuse solar radiations, a tracking system is not required. Their simpler mechanical structure, compared to concentrating collectors, leads to a lower cost which along with little maintenance requirement, are the main advantages of flat plate collectors. The major application of flat plate collectors includes solar water and space heating, solar air conditioning and solar industrial process heat.

A typical flat plate collector is shown in Figure 5 [12]. Solar radiation is passed through a transparent glazing cover. The transparent cover reduces convection losses from the absorbing plate, since a stagnant air layer is formed in the casing, between the absorber plate and the transparent cover, eliminating forced convection heat losses. Glass is a very common material used for glazing, because glass with low iron content has about 90% transmission of incoming shortwave solar radiation at normal incidence and almost no emission of long-wave radiation [12].

Solar radiation is then absorbed by a selective absorber surface with a high absorptivity. A selective surface is characterized by a high short-wave radiation absorbance and a low long-wave radiation emittance. Therefore, the absorber surface absorbs as much as possible of the solar radiation passing through the transparent cover, while losing heat as little as possible by long-wave radiation.

Short-wave solar radiation absorptivity of a surface changes with the nature and color of the coating and also with the angle of incidence. Although usually black color is used for absorber plates, different color coatings have been discussed in Refs. [17 - 19]. A new low-cost method for manufacturing selective solar absorber surface can be found in Ref. [20]. Copper, aluminum and stainless steel are the most frequently used materials for absorber plates. The surrounding and bottom of the flat plate collector are insulated in order to minimize the thermal losses. Collected heat then is transferred to the transport medium in the fluid tubes. Copper, because of its high corrosion resistance, is the most common material for fluid tubes. The high temperature fluid is carried either for use or storage.

Flat plate collectors can be used in either passive or active systems, using natural or forced circulation mechanism, respectively. Therefore, in an efficient solar collector, incident solar radiation is absorbed and is converted to thermal energy. This thermal energy is then transferred to a working fluid, all with the minimum thermal losses.

Flat plate collectors should be directly oriented towards the equator. They should face south if they are located in the northern hemisphere and otherwise north. The optimum tilt angle for flat plate collectors is equal to the latitude of the installation site with 10-15^{o} more or less variation [14].

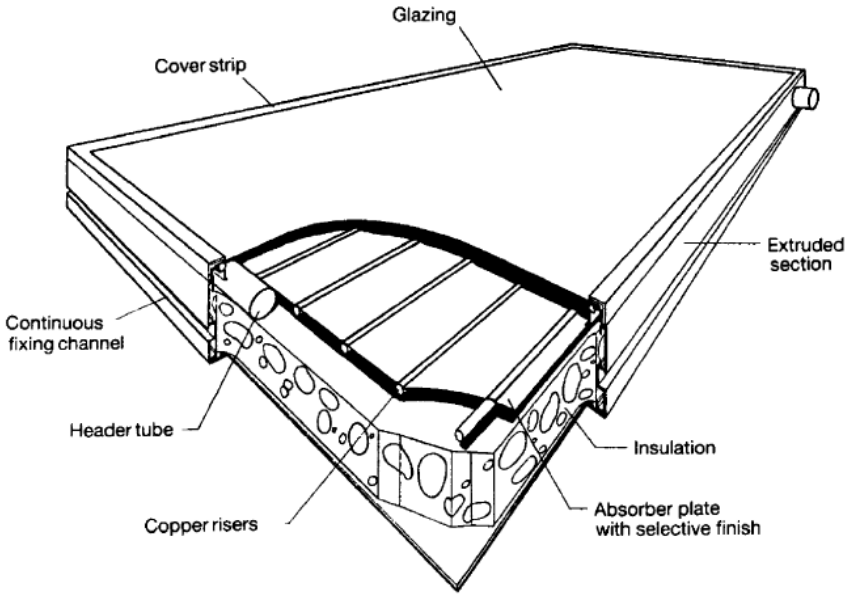

Figure 5: A Typical Flat Plate Collector [12]

As it was mentioned earlier, flat plate collectors are usually fixed in position and don't require a tracking system. This reduces the initial and also the maintenance costs and increases the reliability of flat plate collectors. Due to their advantages, flat plate collectors by far are the most used type of solar collectors. They can be employed for heating both air and water.

They can be used in applications with the low temperature requirements up to 100^{o}C, although slightly higher temperatures could be achieved with some new types of these collectors [21].

2.3.2 Compound Parabolic Collectors

Compound parabolic collectors (CPC) are non-imaging concentrating collectors. In concentrating collectors, the sun radiation is focused by a large collector surface to a smaller receiver surface. In non-imaging collectors, unlike traditional imaging-collectors, imaging the sun onto the receiver is not attempted.

Instead, the focus is on concentrating the solar radiation at the entry area being concentrated upon the receiver. So in non-imagine concentrating collectors, imaging characteristics of the collector are not of concern [22]. CPC can reflect all of the incident radiation to the absorber over a wide range. Winston pointed out these collectors as a potential solar energy collector [23].

A typical sketch for the CPC with a cylindrical absorber is shown in Figure 6 [3]. It includes two reflective surfaces with parabolic profiles (BD and CE), however the lower portions (AB and AC) are circular. Each parabola extends until its surface is parallel with the CPC axis. The side walls are either made of or coated with reflective materials. Some metals with high reflectivity are stainless steel [24-26], aluminum [26], aluminum platting [26,27] and Nickel-Gold platting [28]. Upper parts of the reflective surfaces don't contribute much to collecting and reflecting the solar radiation onto the absorber, thus usually they are truncated, which in turn, decreases the cost of CPC. The solar radiation enters the collector through the aperture. Absorber-receiver has not to be necessarily cylindrical and could be flat, wedge etc. The concentration ratio (C) is defined as the ratio of the aperture area (A_a) to the receiver-absorber area (A_r):

$$C = \frac{A_a}{A_r}$$

Which is always greater than 1 in concentrating collectors and is equal to 1 in flat plate collectors. The acceptance angle ($2\theta_c$) is an angle through which sun can move and still its radiation is converged at the absorber. Acceptance angle of a CPC solar collector is a very important parameter for optimizing the collector's orientation and also employing a suitable tracking system.

Increasing the acceptance angle enables the collector to collect diffuse radiation, while it reduces the concentration ratio. Generally, CPCs with smaller concentration ratios (less than 3) are more interesting in practice. With these concentration ratios, they can accept and concentrate large amounts of incoming diffuse radiation without any tracking system requirement [29].

So it could be concluded that CPCs are designed in such a manner that high concentration is obtained with no need for tracking, because for a specific concentration, the maximum possible angular field of view is achieved [30]. Therefore, non-tracking system is preferable, unless high concentration is significant. By using non-tracking solar collectors, some disadvantages of tracking systems such as advanced control requirements, operating costs, maintenance, complexity of design and etc. could be avoided. A comparison between the conventional stationary CPC solar collector and the single axis tacking CPC solar collector shows that the thermal efficiency of the tracking CPC solar collector is about 14.9% higher than that of the stationary CPC solar collector [31]. With two axis tracking CPC solar collector much more efficiencies are achievable [32].

A CPC concentrator can be oriented with its long axis along either the north-south or the east-west direction with its aperture directly facing towards the equator. The tilt angle is equal to the local latitude.

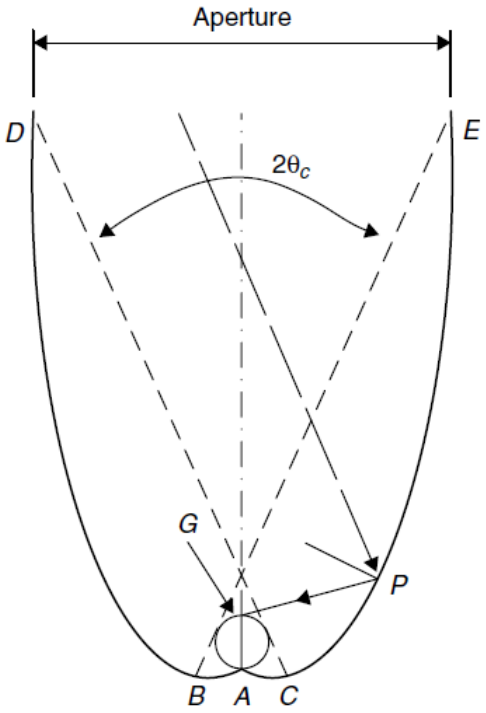

Figure 6: Schematic Diagram of a Compound Parabolic Collector [3]

Ref. [33] presents a method for estimating the optical and thermal properties of a CPC. A parametric analysis shows that the increase in the mass flow rate of the transport medium increases the efficiency of the collector, while decreasing the outlet temperature from the concentrator [34]. Another study shows that when a relatively long tube is used as the absorber of the solar collector or the inlet temperature of the cooling fluid increases, the outlet temperature of the cooling fluid and the daily efficiency decrease [33].

Some researches indicate that under the same testing conditions, the heat losses from flat plate collectors are up to 32% higher compared to a CPC solar collector [35]. CPCs can reach temperatures in the range of 250^{o}C and are simple and reliable in design and operation [16].

2.3.3 Evacuated Tube Collectors

In addition to flat plate collectors, another type of solar collectors is mainly used for solar water heating application, which is called evacuated tube collector. Like flat plate collectors, evacuated tube collectors also collect both direct and diffuse radiations. Comparing with flat plate collectors, evacuated tube collectors reduce convection and conduction thermal losses. Because, as it was mentioned earlier, in flat plate collectors, air is stagnated between the cover and the absorber plates, while in evacuated tube collectors, the absorber surface is located in a glass vacuum-sealed tube. So, convection heat losses are eliminated.

Figure 7 shows a schematic diagram of an evacuated tube collector [12]. A sealed heat pipe, which is a highly efficient thermal conductor, like a copper, contains a small amount of some fluid (for example it could be methanol). This pipe is placed inside a vacuum-sealed tube. Inside the tube, a black copper fin, which acts as an absorber, is attached to the copper pipe.

At the end of the heat pipe, outside of the tube, is a metal condenser attached to the heat pipe. The fluid, inside the heat pipe, is evaporated by the solar heat and the vapor goes to the condenser. These metal condensers are all placed in the manifold which a working fluid like water flows through. Working fluid collects the latent heat of the vapor inside the heat pipe. As a result, vapor condenses and condensed fluid returns back to the solar collector and the process repeats as a cycle. The working fluid, in the manifold, picks up all the heats from the tubes and is heated. This heated liquid can be stored or used.

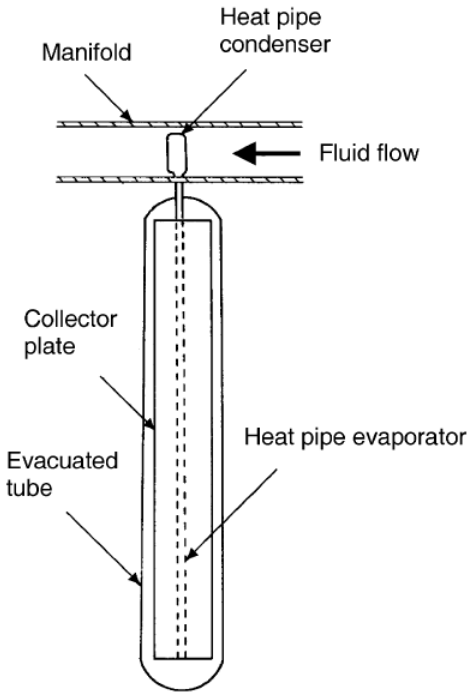

Figure 7: Schematic Diagram of an Evacuated Tube Collector [12]

In evacuated tube collectors, eliminating the convection heat losses and deploying a selective surface at the same time, results in good performance at high temperatures [12]. Reduction in convection and conduction heat losses in vacuum tubes makes it possible for evacuated tube collectors to operate at higher temperatures, compared with flat plate collectors. Although evacuated tube collectors also collect both beam and diffuse radiations, compared with flat plate collectors, they have a better performance at low incidence angles. As a result, in day-long operation, using evacuated tube collectors has an advantage. Conventional flat plate collectors were designed for use in sunny days. They performance suffers greatly with unfavorable conditions like cold, cloudy or windy climate. In these collectors, optical efficiency decreases in the mornings and in the afternoon hours. However, the geometry of an evacuated tube collector makes its absorber be exposed to quasi-normal incidence angle for a longer interval during the day.

Hence, when a standard glazed flat plate collector and an evacuated tube collector were installed and tested at the same working conditions, the evacuated tube collector demonstrated higher efficiency for a wider range of operating conditions [36].

A lot of different evacuated tube collectors with various absorber shapes are available [37]. Several manufactures also have supplied the market with the evacuated tube collectors with CPC-reflectors. Another new design of evacuated tube collector is called integrated compound parabolic collector (ICPC). In this design, a reflective material is fixed at the bottom part of the glass tube [38]. In this way, advantages of the vacuum insulation against thermal losses and non-imaging stationary concentration are combined and used simultaneously in one single collector. Also tracking ICPCs have been devolved for high temperature applications [39].

It is very important to decide whether an evacuated tube or a flat plate collector should be chosen for a specified application. These two collector types have different cost and performance specifications. Therefore, in order to optimize the behavior of the entire system, the energy savings and financial investments, a correct choice is necessary. For energy saving consideration, temperature level required by the specific application and the climate conditions of the installation site should be considered. So, regarding the efficiency, each collector is most favorable for a certain application. A detailed comparative study regarding thermal performance of flat plate and evacuated tube solar collectors in stationary and daily conditions is presented in Ref. [36].

2.4 Solar Energy Storage

Solar energy is a time-dependent energy source. Usually, daily energy demand is also time-dependents and varies during the day. Therefore, at some times, available solar radiation exceeds the thermal energy demand, while at some other occasions there is a lack of solar energy radiation. Figure 8 demonstrate an example of time-dependent profiles of available solar energy and thermal loads [8]. Dashed line represents $\dot{L}$, the thermal load in kW, which is also time-dependent. $\dot{G}_T$ and $\dot{Q}_U$ represent incident solar energy and collector useful gain in kW, respectively.

As it can be seen, during some hours, available energy exceeds the load, while at other times it is less. If a thermal storage system is employed to store extra available solar energy and use it in the times that solar radiation is not available, daily fraction of the thermal load met by the solar system will increase considerably, resulting in less auxiliary energy input requirement.

In this case, vertical shaded areas in Figure 8 show time periods that excess energy is stored and horizontally shaded areas show the occasions in which stored thermal energy is used to meet loads.

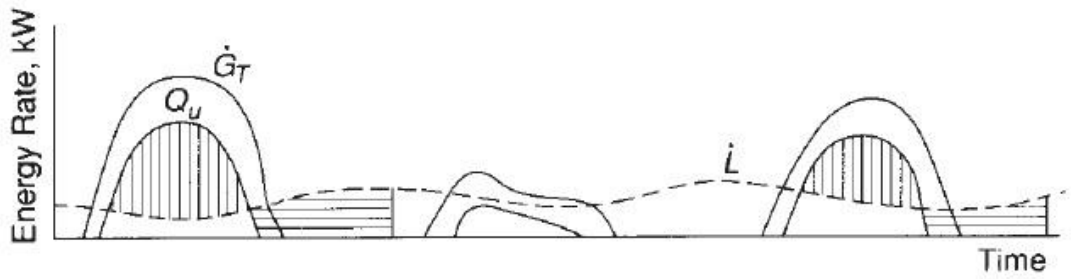

Figure 8: A Time-Dependent Profile of Available Solar Radiation and Thermal Load for a Three-Day Time Period [8]

Therefore, the function of a thermal storage system is to add heat to a storage medium for use at another time. For solar applications, high-temperature storage is typically associated. Energy maybe charged, stored and discharged over various periods of time such as daily, weekly, annually or seasonally [40].

If a thermal storage system is designed and installed properly, it can beneficial in several ways, like shifting loads from peak to nonpeak times, reducing operating or initial costs, providing back-up capacity, extending the capacity of an existing system and more. Thus, designing an efficient energy storage system in solar thermal applications is a matter of great importance. In designing thermal storage systems, three main aspects should be considered [41]: technical, financial and environmental aspects.

For technical considerations, for instance, in order to reduce the storage system size, a high thermal storage capacity is necessary. Also a good heat transfer rate between the heat storage material and heat transfer fluid is important to be able to exchange heat at the required rate. For cost effectiveness, the payoff period of the investment is highly important. Storage material, land and heat exchanger costs are the tree main parts of a storage system cost. Many low-cost materials can be used for solar thermal energy storage [42-44]. Also, several heat transfer enhancement technologies have been developed in order to reduce the associated costs.

Finally, in the design of a solar thermal energy storage system, some criteria should be considered regarding the environmental impact of the system, such as operation strategy, maximum load etc.

A review of different categories of solar thermal storage systems, discussing design criteria, materials used and also different heat transfer enhancement technologies, has been presented in Ref. [45].

2.5 Previous Research on Compound Parabolic Collectors

Compound parabolic collectors have been the subject of many recent researches. Generally, CPCs can be roughly placed in two main categories: two dimensional (2D) and three-dimensional (3D). A 2D CPC has a longitudinal axis, while the geometry of a 3D CPC is obtained by rotating a 2D meridian section of CPC at an angular interval. CPCs can be symmetric or asymmetric. Figure 9 shows some examples of 2D and 3d CPCs [30].

Many researchers have studied the optical performance of different 3D CPCs. The optimization of faceted CPCs was studied by Timinger et al [46]. He discretized the curvature in both the circumferential and axial directions. van Dijk, et al. [48] research involved simulating the relationship between transmission and concentration ratio of circular, square and hexagonal concentrators with reflectance of 95%. The results indicate that as the number of CPC's aperture sides increases, the optical performance approaches more close to ideal transmittance. Cooper et al.'s [48] study also yielded similar results. In this research, researchers compared the optical properties of CPCs with polygonal apertures with 3, 4, 5, 6, 8, 12 sides and circular aperture.

Dielectric CPC is used to enlarge the acceptance angle of a CPC for the same geometry. In this type of CPC, the collector is filled with a dielectric material. The law of refraction implies that by increasing the refractive index of the dielectric, the maximum values of both internal and external acceptance angles for a dielectric-filled

CPC, under total internal reflection conditions at certain refractive indices, will increase [49]. For dielectric filled CPC, materials like clear polyurethane [50-51], PMMA (poly methyl methacrylate) also called acrylic [52], borosilicate glass [53] and other common optical materials in useful visible and infrared region are applicable, as the dielectrics depending on the requirements of refractive index.

CPCs are mostly manufactured using Computer Numerical Control (CNC) technology. As an alternating approach, Van Dijk et al. [47] used 3D-printing successfully to manufacture several CPCs in various shapes and in high fabrication accuracy. CPCs, especially dielectric CPCs, could be also fabricated accurately using modeling. CPCs with more complicated shapes also could be manufactured using modeling.

Thermal performance of CPCs in a solar power plant in Puerto Rico were studied by Oritiz-Rivera and Feliciano-Cruz [54]. According to their study, CPCs collected more solar radiation in sunny days. However, in cloudy days, the power output decreased.

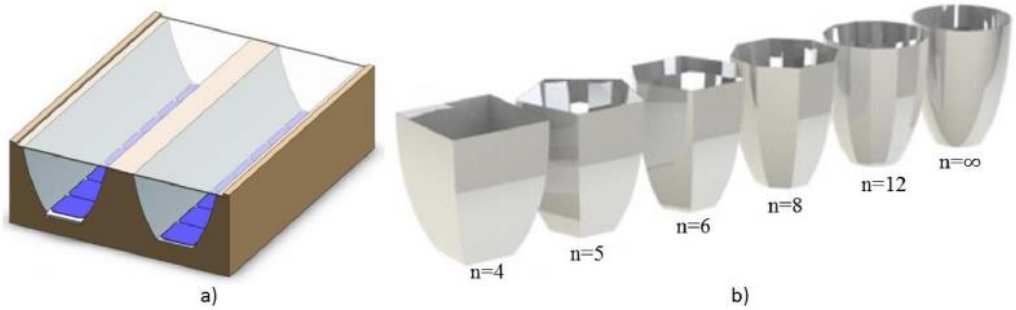

Figure 9: Examples of 2D and 3D CPCs, a) 2D b) 3D with Polygonal Aperture of 4, 5, 6, 8, 12 Sides and Revolved CPC (n=∞) [30]

Their results revealed that the power generation would decrease greatly in a case that the sun is missing for a long time. After long enough absence of the sun, the power generation could even reduce to zero.

Different geometries for the absorber have been investigated. A prototype performance of 2D trough CPC with a flat absorber on base was examined by Al-Ghasem et al. [55]. The measurements were carried out under Jordan, Irbid climate, from March to May in 2013. Results showed that, compared with a stationary CPC, the highest temperature of the absorber in a tracking CPC increased up to 27.7% in March. Although the cost of the tracking system also should be considered.

Mishra et al. [56] integrated the U-shaped evacuated tabular collector with compound parabolic concentrator to optimize the evacuated tabular collector. Ratismith et al. [57] devised two innovative CPCs, both having a double sided absorber plate in the middle. One is double-parabolic trough and the other is flat-base trough. Results showed that flat-base trough with its double sided absorber plate aligned vertically, had a higher efficiency compared with double-parabolic trough with horizontal alignment of absorber.

Abdullahi et al. [58-59] compared the performance of four CPC collectors with different absorbers as is shown in Figure 10. The ones with two receivers aligned horizontally and with elliptically shaped receivers, showed 15% and 17% increase in the daily optical efficiency respectively, compared with conventional collector with one tabular receiver.

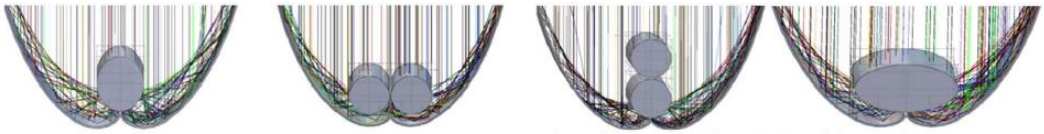

Figure 10: Four CPC Solar Thermal Collectors with Different Absorbers [57]

Moreover, the collector with double tube receivers demonstrated a better performance in heat transfer to the cooling water, compared with a collector with single receiver.

A small scale Organic Rankine Cycle (ORC) plant was proposed by Antonelli et al. [60]. In this plant CPCs were used as a heat source and a volumetric machine was utilized as an expander. A traditional trough CPC reflector was used with a tabular absorber at the bottom. The maximum energy produced with the concentration ratio between 1.1 and 1.4 and the tilt angle smaller than 20-25^{o}.

Tiwari et al. [61] used a recuperated organic Rankine cycle integrated with a novel glazed reverse absorber conventional compound parabolic concentrator (GRACCPC). The collector contained low global warming potential and zero ozone depletion potential mixture of cyclohexane/R245fa as a working fluid. The outlet temperature of the collector could reach 398K at noon.

Compound parabolic collectors are subject to many researches. Future work on CPCs may include improving several aspects including geometry, manufacturing, tracking systems, thermal performance, etc.

Although CPCs have received a lot of attention from researchers in recent years and many experimental and numerical studies have been carried out on this type of solar collectors, usually CPCs with relatively high truncation ratios are the subjects of

studies, which are proper for medium-temperature industrial application. Thus, not too much information is available on the performance of CPCs in low temperature residential heating applications. This study is aimed to investigate the potential of a small scaled CPC with low truncation ratio for being utilized in a residential solar water heating system. Hot water is then stored in a storage tank and could be used for space heating and/or domestic hot water requirements. Using a CPC with a low truncation ratio makes it possible to replace existing flat plate collector with the CPC. The study compares the performance of CPC with that of flat plate collector. Moreover, this study has been done for two different cities, one with abundant and the other with limited solar radiation, to distinguish between the performance of the CPC in climates with high and low beam radiations.

Chapter 3

SYSTEM AND MATHEMATICAL MODEL

3.1 Solar Water Heating System

A schematic of a simple solar water heating system is shown in Figure 11. The system includes some main components. The main components are discussed below:

Solar Collector: Solar collector is the main component of any solar water heating system and is used to collect the solar radiation. After converting it to thermal energy, solar thermal energy is transferred to a working fluid with the minimum heat loss. In this study thermal performance of a flat plate collector and a compound parabolic collector are studied numerically and then compared.

Pump: In active solar systems, flow is maintained by a pressure difference in the system. Pumps are used to cause the pressure difference in the system and circulate fluid in two separate loops, one loop for collector and the other for the tank.

Storage Tank: Usually it is better to store the thermal energy for the cases that either the sun radiation is not available or auxiliary energies are at peak rates. Storage tank is used to store the thermal energy. Energy is stored and removed from this storage tank at a desirable rate. If available solar gain is not enough to meet thermal loads, the auxiliary heater will supply more heating to maintain the tank outlet temperature at the defined set point temperature. In this study an unstratified or fully mixed tank is used in the simulation.

The model optionally includes an electric heating element, subject to temperature control. The control option allows the heater to operate during times that the available solar energy is not adequate to meet the thermal load. The auxiliary heater employs a temperature dead band. The heater is enabled if the temperature of storage tank is less than $T_{set} - \Delta T_{db}$, where T_{set} is the set point temperature and ΔT_{db} is the dead band temperature difference.

Pipelines: Pipelines connect the collector to the thermal storage tank. Transport medium transports the heat from the collector to the storage tank. Fittings and the equipment for filling and emptying are another components of a solar heating water system.

Differential Controller: A differential controller is used to control the operation of the pump. With an on-off controller, the circulating pump is turned on when the collector supplies enough output. Usually the controller employs two temperature sensors, one in the bottom of the storage tank and the other at the exit of the collector. When the measured temperature deference falls below a certain amount, the pump will be turned off by the controller.

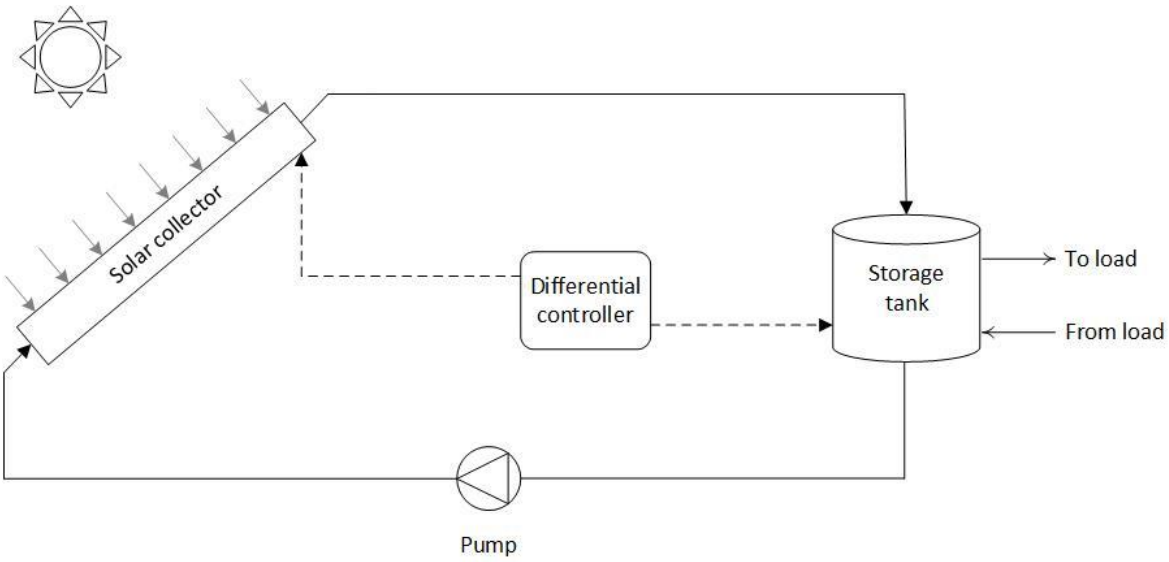

Figure 11: A Typical Solar Water Heating System

3.2 Mathematical Model

3.2.1 Compound Parabolic Collector

There are several models in order to describe the thermal performance of a CPC mathematically. In this section, the mathematical formulation used by TRNSYS version 16.01.0003 for modeling CPCs will be reviewed [62]. Also, a MABLAB code for modeling a CPC has been provided in Appendix A.

TRNSYS models a CPC with a flat absorber, as shown in Figure 12, in which θ_c is half-acceptance angle. A CPC collects both beam and diffuse radiation, which approaches the aperture within a critical angle θ_c, the half-acceptance angle. A full CPC is the one in which the walls extend upward to a height which gives an aperture area of $1/\sin\theta_c$ times the absorber area.

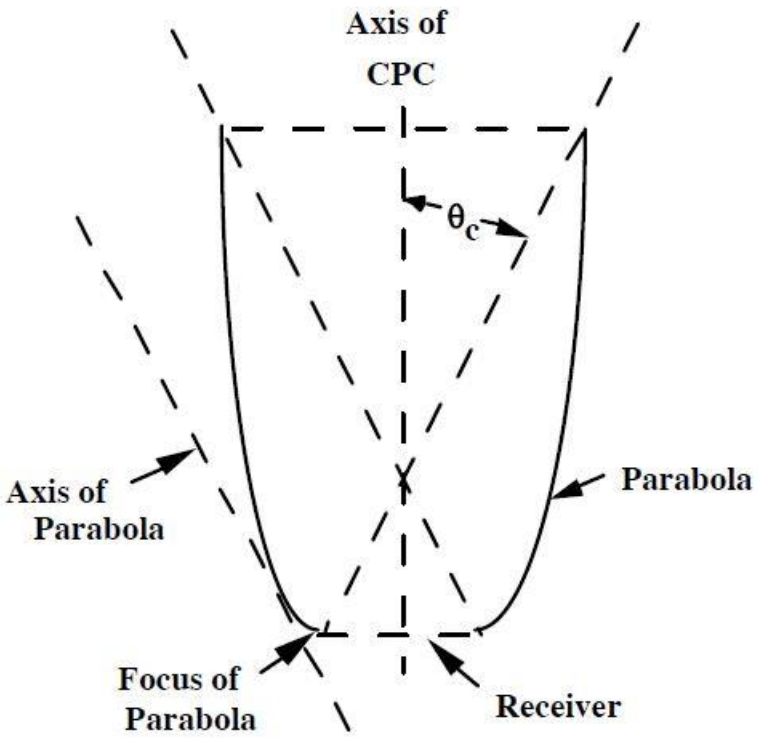

Figure 12: A CPC Design Modeled in TRNSYS [62]

Optimal concentration is achieved in a full CPC, but a very large reflector area in required. In practice, most CPC's are truncated to a height smaller than that of the full CPC.

There are two possible orientations for a CPC receiver. In the first orientation, longitudinal plane, the CPC axis may be located in a vertical plane that contains the surface azimuth. Beam radiation enters the CPC whenever $\theta_l < \theta_c$ where:

$$\theta_l = \left|\tan^{-1}(\tan\theta_z \cos(\gamma - \gamma_s)) - \beta\right| \quad (3\text{-}1)$$

In other case, The CPC receiver maybe located in a transverse plane 90° from the longitudinal orientation. In this case, beam radiation enters the CPC when $\theta_t < \theta_c$ where:

$$\theta_t = \tan^{-1}\left(\frac{\sin\theta_z \sin(\gamma - \gamma_s)}{\cos\theta}\right) \tag{3-2}$$

View factors to the sky and ground are used to estimated diffuse radiation entering the aperture. For the longitudinal receiver orientation:

$$F_{sky} = \frac{1+\cos\beta}{2C} \tag{3-3}$$

$$F_{gnd} = \frac{1-\cos\beta}{2C} \tag{3-4}$$

And for the transverse receiver orientation:

$$F_{sky} = \frac{1/C + \min(1/C, \cos\beta)}{2} \tag{3-5}$$

$$F_{gnd} = \frac{\max(1/C, \cos\beta) - \cos\beta}{2} \tag{3-6}$$

Using the X-Y coordinates, like the ones shown in Figure 13, the equation of a branch of CPC could be written as:

$$Y = \frac{X^2}{2s(1+\sin\theta_c)} \tag{3-7}$$

Which s is the absorber width. Figure 24 in Appendix B provides a detailed geometrical description of a CPC. The X-coordinate of the endpoint of the branch is:

$$X_s = s\cos\theta_c \tag{3-8}$$

and

$$\overline{X} = s\left[\frac{1+\sin\theta_c}{\cos\theta_c}\right]\left[-\sin\theta_c + (1+\frac{\overline{h}}{h}\cot^2\theta_c)^{1/2}\right] \tag{3-9}$$

Which h is the height of the full CPC. The concentration ratio of the CPC is found by:

$$C = \frac{A_a}{A_r} = 2(\frac{\overline{X}}{s})\cos\theta_c - (\frac{\overline{X}}{s})^2 \frac{\sin\theta_c}{\sin\theta_c + 1} + \sin\theta_c - \cos^2\theta_c \tag{3-10}$$

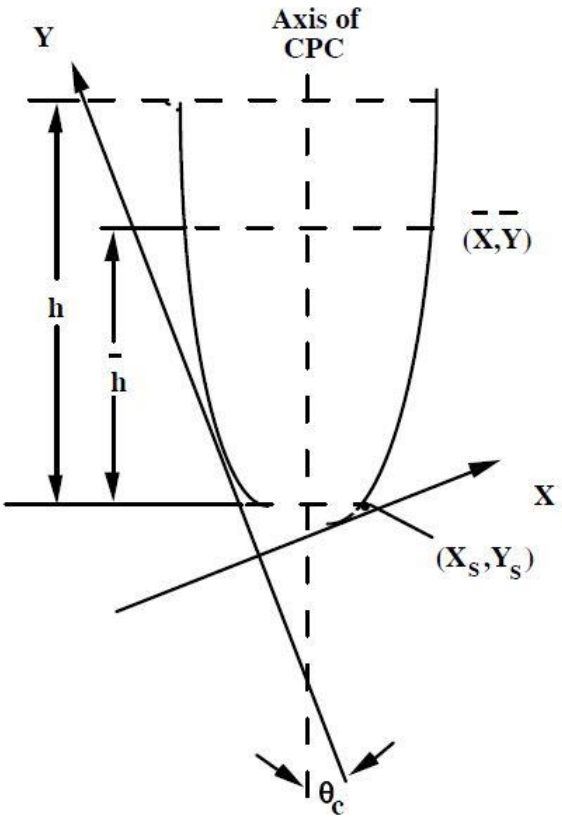

Figure 13: X-Y Coordinates Used in Formulation of the Compound Parabolic Collector in TRNSYS [62]

For a full CPC, $\bar{h}/h=1$, the concentration ratio is $1/\sin\theta_c$. The concentration ratio falls of by truncating the CPC.

n_r, the average number of internal reflections, could be expressed as:

$$n_r = \frac{A_{ref}}{A_r}\left(\frac{1}{2} - \frac{\overline{X}^2 - X_s^2}{2A_{ref}\,s(1+\sin\theta_c)}\right) \tag{3-11}$$

A_{ref} is the reflector's area and is found as:

$$\frac{A_{ref}}{A_r} = (1+\sin\theta_c)\ln\left[\frac{\frac{\overline{X}}{s}+\sqrt{(1+\sin\theta_c)^2+(\frac{\overline{X}}{s})^2}}{\cos\theta_c+\sqrt{2(1+\sin\theta_c)}}\right] + \frac{\overline{X}}{s}\sqrt{1+\left(\frac{\overline{X}}{s(1+\sin\theta_c)}\right)^2} \tag{3-12}$$

$$-\frac{\cos\theta_c\sqrt{2}}{\sqrt{1+\sin\theta_c}}$$

The CPC absorber is modeled using the Hottel-Whillier model collector such that:

$$\dot{Q}_u = A_a F_R[\mathrm{I}_T(\mathrm{TA}) - U_L(T_i - T_a)] \tag{3-13}$$

Which U_L is overall loss coefficient per unit aperture area and F_R is the collector heat removal factor and is given by:

$$F_R = \frac{\dot{m}C_p}{A_a U_L}[1 - \exp(-\frac{A_a U_L F'}{\dot{m}C_p})] \tag{3-14}$$

And the overall transmittance-absorbtance product, (TA), is calculated as:

$$(\mathrm{TA}) = \frac{(\tau\alpha)_b F_b I_{bT} + (\tau\alpha)_d I_d F_{sky} + (\tau\alpha)_g \rho_g I F_{gnd}}{I_T} \tag{3-15}$$

Where F_b is a control function so that $F_b = 1$ if the sun is within the acceptance angle, and $F_b = 0$ otherwise. Also, I_{bT} is the beam radiation normal to the aperture area and could be found by:

$$I_{bT} = I_T - I_d \frac{1+\cos\beta}{2} - \rho_g I \frac{1-\cos\beta}{2} \tag{3-16}$$

$(\tau\alpha)_b, (\tau\alpha)_d$ and $(\tau\alpha)_g$ in (3-15) are the product of the cover transmittance and the absorber absorptance for beam, diffuse and ground reflected radiations respectively. Only part of the diffuse and ground reflected radiations effectively enter the CPC, and this is a function of the acceptance angle. Using the isotropic diffuse model on an hourly basis, the relationship between the diffuse and ground reflected effective incidence angle and the half acceptance angle is given by:

$$\theta_d = \theta_g = 44.86 - 0.0716\theta_c + 0.00512\theta_c^2 - 0.0000798\theta_c^3 \tag{3-17}$$

$(\tau\alpha)_d = (\tau\alpha)_g$ in (3-15) are calculated at diffuse and ground reflected effective incidence angles $\theta_d = \theta_g$, so (3-15) could be written as:

$$(\mathrm{TA}) = \frac{(\tau\alpha)_b F_b I_{bT} + (\tau\alpha)_d \left[I_d F_{sky} + \rho_g I F_{gnd} \right]}{I_T} \tag{3-18}$$

All transmittance-absorbance products are determined using an effective absorbtance:

$$\alpha_{eff} = \rho_{eff} \alpha \tag{3-19}$$

Where $\rho_{eff} \approx \rho_R^{n_r}$, in which ρ_R is the wall reflectance and n_r is the average number of internal reflections, given by (3-11).

The procedure for calculating transmittance-absorbance products is as follows:

Fresnel's equations for reflectance at a planar interface for perpendicular and parallel unpolarized radiation are:

$$r_\perp = \frac{\sin^2(\theta_1 - \theta_2)}{\sin^2(\theta_1 + \theta_2)} \tag{3-20}$$

$$r_\parallel = \frac{\tan^2(\theta_1 - \theta_2)}{\tan^2(\theta_1 + \theta_2)} \tag{3-21}$$

θ_1 and θ_2 are related by Snell's Law:

$$\sin\theta_1 = n_g \sin\theta_2 \tag{3-22}$$

Which the index of fraction for air is taken unity.

Allowing for both reflection and absorption losses, cover transmittance perpendicular and parallel components of polarization are:

$$\tau_\perp = \frac{\tau_a (1 - r_\perp)^2}{1 - (r_\perp \tau_a)^2} \tag{3-23}$$

$$\tau_\parallel = \frac{\tau_a (1 - r_\parallel)^2}{1 - (r_\parallel \tau_a)^2} \tag{3-24}$$

Which τ_a is the transmittance when only absorption losses have been considered:

$$\tau_a = \exp\left(-\frac{KL}{\cos\theta_2}\right) \tag{3-25}$$

To find the cover transmittance, the transmittances for the parallel and perpendicular components of polarization are averaged:

$$\tau = \frac{1}{2}(\tau_\perp + \tau_\parallel) = \frac{\tau_a}{2}\left[\frac{(1-r_\perp)^2}{1-(r_\perp\tau_a)^2} + \frac{(1-r_\parallel)^2}{1-(r_\parallel\tau_a)^2}\right] \tag{3-26}$$

Similarly, for reflectance, perpendicular and parallel components of polarization are:

$$\rho_\perp = r_\perp(1+\tau_a\tau_\perp) \tag{3-27}$$

$$\rho_\parallel = r_\parallel(1+\tau_a\tau_\parallel) \tag{3-28}$$

And reflectance of the cover again is found by averaging these components:

$$\rho = \frac{1}{2}(\rho_\perp + \rho_\parallel) = \frac{1}{2}\left[r_\perp(1+\tau_a\tau_\perp) + r_\parallel(1+\tau_a\tau_\parallel)\right] \tag{3-29}$$

ρ_d , the reflectance of the cover for diffuse radiation incident coming from the absorber surface, is obtained by using (3-29) at the diffuse effective incidence angle, θ_d , given by (3-17).

Finally, the transmittance-absorptance product is calculated by:

$$(\tau\alpha) = \frac{\tau\alpha_{eff}}{1-(1-\alpha_{eff})\rho_d} \tag{3-30}$$

By definition, efficiency, η, of a CPC is the ratio of the rate of useful solar energy gain of the collector to the rate of total incident radiation on the aperture plane, that is:

$$\eta = \frac{\dot{Q}_u}{A_a I_T} \tag{3-31}$$

3.2.2 Flat Plate Collector

TRNSYS provides several components for modeling flat plate collectors. In this study, a quadratic efficiency flat plate collector, with 2nd order incidence angle modifiers, has been chosen. In this section, TRNSYS formulation for this type of flat plate collectors is presented [62].

A general equation for solar thermal collector efficiency can be obtained from the Hottel-Whillier equation as:

$$\dot{Q}_u = F_R \, \mathrm{A}_c [\mathrm{S} - U_L (T_i - T_a)] \tag{3-32}$$

$$\eta = \frac{\dot{Q}_u}{A_c I_T} = \frac{F_R \, \mathrm{A}_c [(\tau\alpha)_n I_T - U_L (T_i - T_a)]}{A_c I_T} = F_R (\tau\alpha)_n - F_R U_L \frac{(T_i - T_a)}{I_T} \tag{3-33}$$

F_R is the collector heat removal factor and is given by:

$$F_R = \frac{\dot{m} C_p}{A_c U_L} [1 - \exp(-\frac{A_c U_L F'}{\dot{m} C_p})] \tag{3-34}$$

The loss coefficient U_L is not exactly constant, so a better expression is obtained by taking into account a liner dependency of U_L versus $(T_i - T_a)$:

$$\eta = \frac{\dot{Q}_u}{A_c I_T} = F_R (\tau\alpha)_n - F_R U_L \frac{(T_i - T_a)}{I_T} - F_R U_{L/T} \frac{(T_i - T_a)^2}{I_T} \tag{3-35}$$

Equation (3-20) can be written as:

$$\eta = a_0 - a_1 \frac{(T_i - T_a)}{I_T} - a_2 \frac{(T_i - T_a)^2}{I_T} \tag{3-36}$$

Which is the general solar collector thermal efficiency equation used in the model. The thermal efficiency is defined by 3 Parameters: a_0, a_1 and a_2.

These 3 parameters are available for collectors tested according to ASHRAE (American Society Of Heating, Refrigeration And Air Conditioning Engineers) and rated by SRCC (Solar Rating And Certification Corporation), (ASHRAE, 2003; SRCC, 1995), as well as for collectors tested according to the recent CEN (the European Committee for Standardization) standards on solar collectors (CEN, 2001).

Collector tests are generally performed on clear days at normal incidence so that the transmittance-absorptance product $(\tau\alpha)$ is nearly the normal incidence value for beam radiation, $(\tau\alpha)_n$. The intercept efficacy, $F_R(\tau\alpha)_n$, is corrected for non-normal solar incidence by the factor $(\tau\alpha)/(\tau\alpha)_n$. By definition, $(\tau\alpha)$ is the ratio of the total absorbed radiation to the incident radiation. So, a general expression for $(\tau\alpha)/(\tau\alpha)_n$ is:

$$\frac{(\tau\alpha)}{(\tau\alpha)_n} = \frac{I_{bT}\frac{(\tau\alpha)_b}{(\tau\alpha)_n} + I_d(\frac{1+\cos\beta}{2})\frac{(\tau\alpha)_d}{(\tau\alpha)_n} + \rho_g I(\frac{1-\cos\beta}{2})\frac{(\tau\alpha)_g}{(\tau\alpha)_n}}{I_T} \tag{3-37}$$

For flat plate collectors $(\tau\alpha)_b/(\tau\alpha)_n$ for beam radiation can be approximated from ASHRAE test results (ASHRAE, 2003) as:

$$K_{\tau\alpha} = \frac{(\tau\alpha)_b}{(\tau\alpha)_n} = 1 - b_0\left[\frac{1}{\cos\theta} - 1\right] - b_1\left[\frac{1}{\cos\theta} - 1\right]^2 \tag{3-38}$$

For diffuse and ground reflected radiations $(\tau\alpha)_d/(\tau\alpha)_n$ and $(\tau\alpha)_g/(\tau\alpha)_n$ also could be evaluated from (3-38) at the diffuse and ground reflected radiation effective incident angles θ_d and θ_g:

$$\theta_d = 59.68 - 0.1388\beta + 0.001497\beta^2 \tag{3-39}$$

$$\theta_g = 90.00 - 0.5788\beta + 0.002693\beta^2 \tag{3-40}$$

In most cases, the fellow rate at which test data are measured is not match with the flow rate used in the application. In these cases, a correction ratio, r, is used to correct the tested $F_R U_L$ and $F_R(\tau\alpha)_n$ values:

$$r = \frac{F_R U_L\big|_{use}}{F_R U_L\big|_{test}} = \frac{F_R(\tau\alpha)_n\big|_{use}}{F_R(\tau\alpha)_n\big|_{test}} \tag{3-41}$$

$$r = \frac{\left.\frac{\dot{m}C_p}{A_c}\left[1-\exp(-A_c F' U_L / \dot{m}C_p\right]\right|_{use}}{\left.\frac{\dot{m}C_p}{A_c}\left[1-\exp(-A_c F' U_L / \dot{m}C_p\right]\right|_{test}} \tag{3-42}$$

$$r = \frac{\left.\frac{\dot{m}C_p}{A_c}\left[1-\exp(-A_c F' U_L / \dot{m}C_p\right]\right|_{use}}{F_R U_L\big|_{test}} \tag{3-43}$$

For calculating r, estimating $F'U_L$ is necessary. For the test conditions, it can be obtained by solving (3-34) for $F'U_L$:

$$F' U_L = -\frac{\dot{m}C_p}{A_c}\ln\left(1-\frac{F_R U_L A_c}{\dot{m}C_p}\right) \tag{3-44}$$

The values of $F'U_L$ for the test and use conditions are approximately the same, so the value calculated from (3-44) could be used in both numerator and denominator of (3-42).

3.2.3 Collector Outlet Temperature

The useful solar heat gained is used to raise the collector inlet water temperature from T_i to outlet temperature T_o:

$$\dot{Q}_u = \dot{m}C_p(T_o - T_i) \tag{3-45}$$

$$T_o = \frac{\dot{Q}_u}{\dot{m} C_p} + T_i \tag{3-46}$$

3.2.4 Storage Tank Temperature

An energy balance on an unstratified fully mixed tank gives:

$$(\mathrm{m} C_p)_s \frac{dT_s}{dt} = \dot{Q}_u - \dot{L}_s - (UA)_s (T_s - T_a') \tag{3-47}$$

Where $(\dot{m} C_p)_s$ is the mass flow rate times specific heat on the storage tank side. If we write the temperature derivative as:

$$\frac{dT_s}{dt} = \frac{T_s^+ - T_s}{\triangle t} \tag{3-48}$$

And solve for the tank temperature at the end of a time increment, the temperature at the end of an hour is calculated as:

$$T_s^+ = T_s + \frac{\triangle t}{(mC_p)_s} [\dot{Q}_u - \dot{L}_s - (UA)_s (T_s - T_a')] \tag{3-49}$$

Chapter 4

SIMULATION USING TRNSYS

4.1 TRNSYS Simulation Program

TRNSYS or transient systems simulation program is a widely used software for simulating transient systems. It's a commercial software package developed at the Solar Energy Laboratory at the University of Wisconsin, Madison, over 30 years ago. Although it was originally developed for solar energy applications, now it is used for simulation of a wider variety of thermal processes. TRNSYS is a flexible tool with a graphical interface which could be used to simulate and study a wide range of transient energy systems. It includes subroutines that represent the typical components in solar energy or other energy systems.

TRNSYs is consisted of two main parts. One is the engine and the other is its rich library of components. The engine, which is called kernel, reads the input information and carries out the calculations, in other words, solving the governing equations on the system, and finally provides the user with the results, usually in the form of graphs and plots. The library includes every component might be needed to model and analyses an energy system. The standard library includes more than 100 components ranging from pumps and solar collectors to weather data processors and HVAC (Heating, Ventilating and Air Conditioning) equipment. Extended libraries, including new or improved components are also available.

One of the main reason for TRNSYS success over the last 30 years is its open scours nature. The source code of the kernel as well as the components models are available to the end users. This feature, makes it easy for the user to extends the existing models to make them fit for their specific needs. Furthermore, it is easily possible to add custom component models using all common programming languages such as C++, Fortran etc. Moreover, TRNSYS could be easily connected to many other applications like MATLAB, EES and etc. in order to perform pre- or post-processing.

Currently the 18th version of TRNSYS is available. The program has undergone several major revisions and many more minor changes since the first time it became available in 1977. Continuous improvements and validations over all these years, have made TRNSYS a popular reliable simulation tool in the energy simulation community. More information about TRNSYS and its different versions, features, libraries and etc. could be found at TRNSYS official website at www.trnsys.com. In this study, TRNSYS version 16.01.0003 has been used.

4.2 Modeling a Solar Water Heating System Using TRNSYS

A solar water heating system has been modeled in this study and its performance in the first week of January has been investigated. The simulation has carried out once in Nicosia and another time in London. A flat plate collector and a CPC have been used as the collector of the system, alternatively. Figure 14 and Figure 15 show solar water heating systems, using flat plate collector and CPC, respectively. The components used in the studio and their descriptions are listed in Table 1.

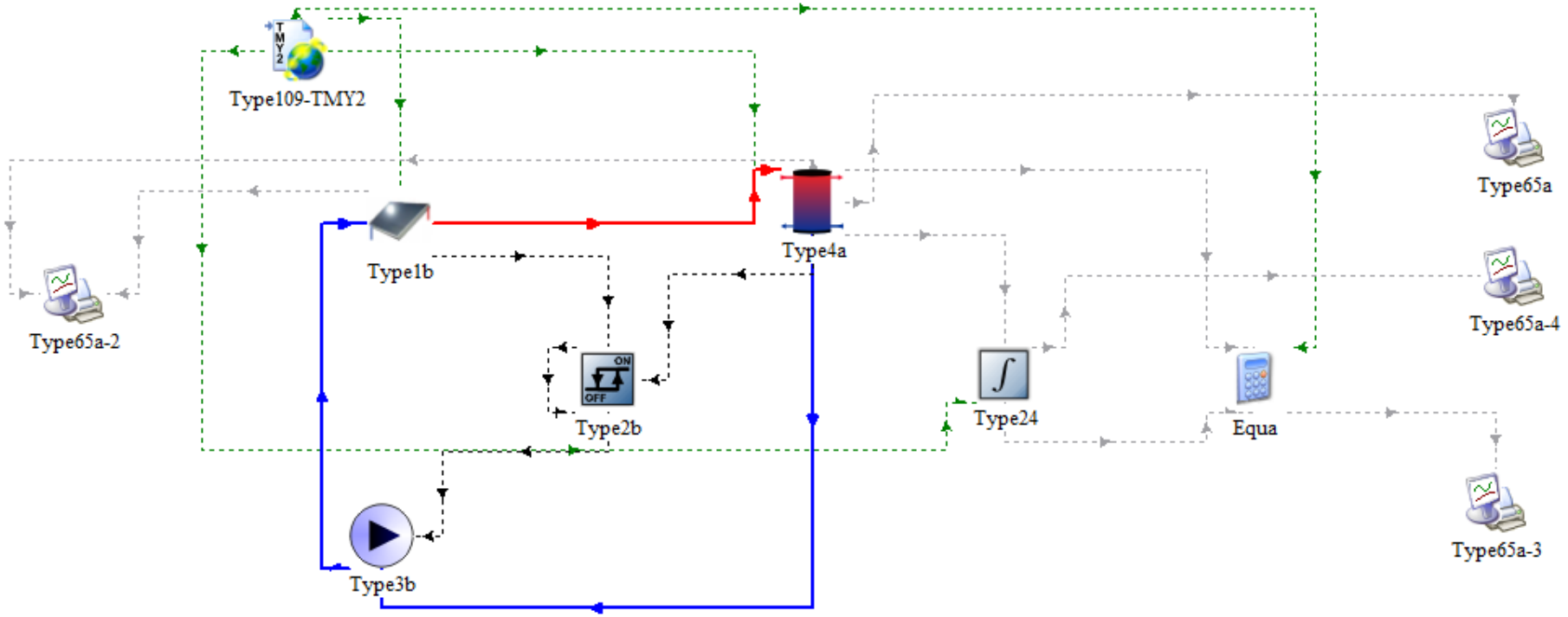

Figure 14: The System Using Flat Plate Collector

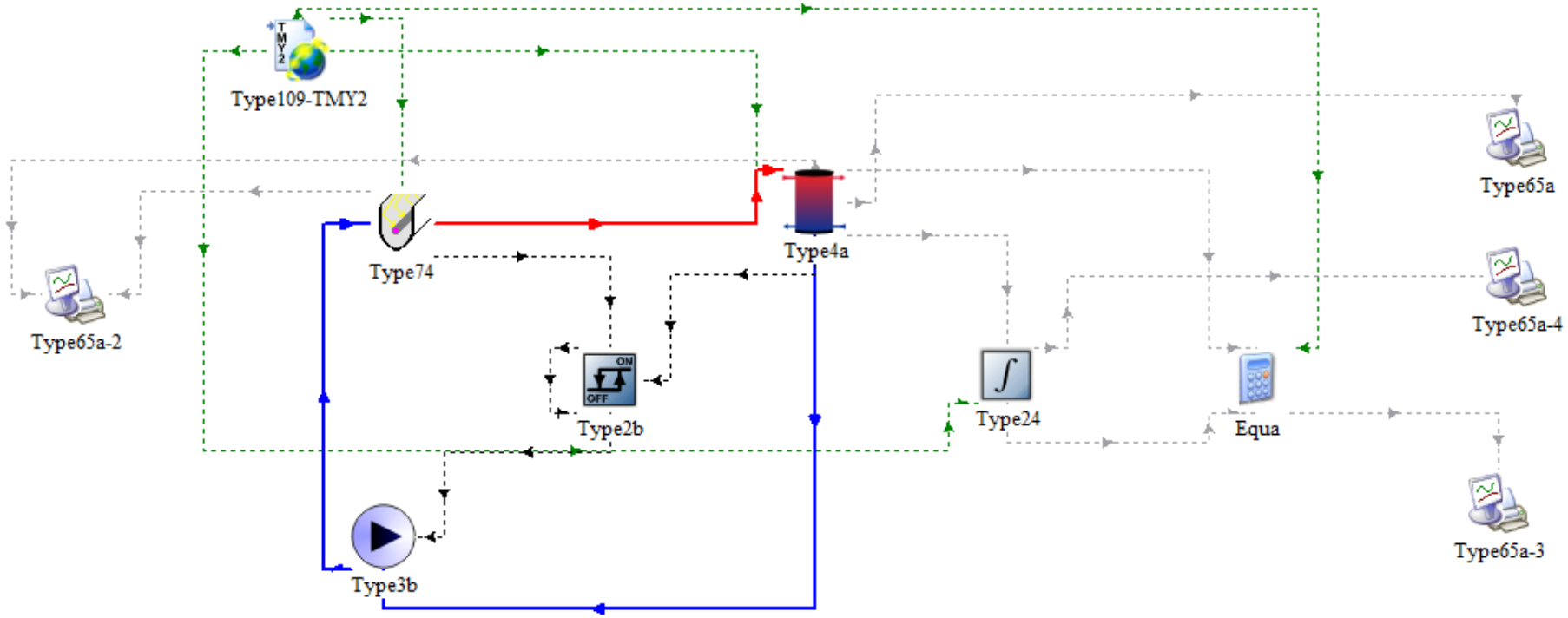

Figure 15: The System Using CPC

Table 1: Components Used in The Simulation Studio

Component (type)	Description
Type109-TMY2	Data reader and radiation processor
Type1b	Solar collector - quadratic efficiency
Type74	Solar collector - CPC collector
Type3b	Pump
Type2b	On/Off differential controller
Type4a	Unstratified storage Tank
Type24	Quantity Integrator
Type65a	Online graphical plotter

An unstratified storage tank (Type4a) is located outdoor and is aimed to provide hot water at a fixed set point temperature of 60^{o}C 24 hours a day throughout the simulation. The tank is fully mixed and the temperature distribution throughout the tank is uniform. The tank is equipped with an electric heater which supplies heat to the water when delivered solar energy from the collector is not sufficient to achieve the desired temperature. A dead band temperature difference of 5^{o}C is set. The thermostat will enable the heating element when the tank temperature falls below the set point temperature by this amount.

A pump (Type3b) is used to maintain the flow through the pipe work. The operation of the pump is controlled by a differential controller (Type2b). This controller reads two input temperatures. The lower input temperature reads the temperature of the tank and the upper input temperature reads the collector outlet temperature. If the collector outlet temperature falls below the tank temperature, the controller turns the pump off and prevents the fluid to circulate and loos heat.

Table 2: CPC Parameters

Parameter	Value
Collector aperture area (m^2)	2
Fluid specific heat ($J/kg-K$)	4190
Collector fin efficiency factor (-)	0.92
Collector overall heat loss coefficient (W/m^2-K)	2.5
Collector wall reflectivity (-)	0.9
Collector half-acceptance angle (-)	35
Truncation ratio (-)	0.1
Absorptance of absorber plate (-)	0.87
Axis orientation	Transverse
Fluid mass flow rate (kg/s)	0.02

Table 3: Flat Plate Collector Parameters

Parameter	Value
Collector area (m^2)	2
Fluid specific heat ($J/kg-K$)	4190
Collector intercept efficiency (-)	0.8
Collector efficiency slope (W/m^2-K)	3.61
Collector efficiency curvature (W/m^2-K^2)	0.05
Collector 1st-order incidence angle modifier (-)	0.2
Collector 2nd-order incidence angle modifier (-)	0
Fluid mass flow rate (kg/s)	0.02

In this study no thermal load is considered and the focus is on the tank temperature variations due to the flat plate collector and CPC performances. Thus, just hot water from the collector circulates through the storage tank and returns to the collector.

Table 4: Storage Tank Parameters

Parameter	Value
Storage tank capacity per collector area (kg / m^2)	75
Tank Volume (m^3)	0.15
Tank loss coefficient ($W / m^2 - ^\circ C$)	0.8
Set point temperature ($^\circ C$)	60
Dead band for heating element ($^\circ C$)	5

Type1b and Type74 model a quadratic efficiency flat plate collector with 2nd order incidence angle modifiers, and a CPC, respectively. The CPC has a flat absorber, as shown in Figure 12. Figure 25 in Appendix B shows a drawing of the simulated CPC, with the related dimensions. Table 7 in Appendix B also lists the dimensions of the corresponding CPC, calculated using the MATLAB code provided in Appendix A. The values in Table 7 have been calculated using the parameters given in Table 2.

Type109-TMY2 is used to read weather data at regular time intervals from a data file. This component converts the data to a desired system of units and processes the solar radiation data in order to calculate radiation on a tilted surface and angle of incidence for an arbitrary surface. Type109-TMY2 reads a weather data file in the standard TMY2 format.

Type24 integrates a series of quantities over a period of time. As an instance, if total useful heat collected by the collector over the year is needed, hourly data will be send to this component and integrated. The result could be used for more calculations or could be send to a plotter. Equa is a tool is used to calculated any equation with either constant parameters or output of other components.

Finally, a plotter (Type65a) displays the selected system variables while the simulation is progressing. Table 2 to Table 4 list the parameters used in the simulation.

In both cites collectors are installed with a slope equal to the latitude of the installation site, 35^{o} N for Nicosia and 52^{o} N for London. Also, in both cities collectors face south, with the azimuth angle of zero. In order to compare the performance of two collectors, both collectors have a same fluid mass flow rate and area.

A full CPC for two main reasons is not suitable for domestic applications. Firstly, it will be too large and this makes the installation difficult, so that replacing a typical flat plate collector with a large CPC might not be practical and feasible in solar hot water applications. Secondly, a full CPC has a high performance only when it is oriented properly to let enough sunlight enters the aperture, which this optimum orientation changes during the day as sun's position changes in the sky. As a result, as sun's position in the sky varies, not enough radiation enters the full CPC. However, a truncated CPC will let more sun light enters the aperture during the day. Thus, in this simulation a truncated CPC with a very small truncation ratio is considered to let more sunlight enters the aperture during the day.

Simulation time step is taken 1 hour to show hourly variations of related physical quantities. Simulation will be run for the first week of January and both discrete and cumulative data will be calculated and displayed.

Chapter 5

RESULTS AND DISCUSSION

In this chapter results of simulating a solar heating water system containing a storage tank and a solar collector will be presented. The aim is to model the system and investigate the temperature variations of the tank, and calculate the weekly auxiliary power required to maintain the tank temperature at 60^{o}C over 24 hours a day during all week. The simulation is carried out for two types of solar collectors, a conventional flat plate collector and a CPC. The geometry and design of the CPC is chosen in a way that it can be used in a domestic solar hot water system instead of a flat plate collector.

Also, simulation is repeated for two cities, one Nicosia with abundant yearly available solar radiation, and the other, London, with relatively less available total and beam radiations. All simulations have been accomplished for one-week duration, with time step of 1 hour. In other words, the behavior of the system is calculated for every hour, for one week. The performances and related quantities for flat plate collector and CPC are compared. Required auxiliary power requirement determined how much energy should be purchased for water heating purposes.

Figure 16 shows beam, diffuse and total radiations striking the collector surfaces, in Nicosia and London for the first week of January. As it is observable, even during the winter rime, relatively high amounts of solar radiations are available in Nicosia. However, diffuse radiation exceeds beam radiation.

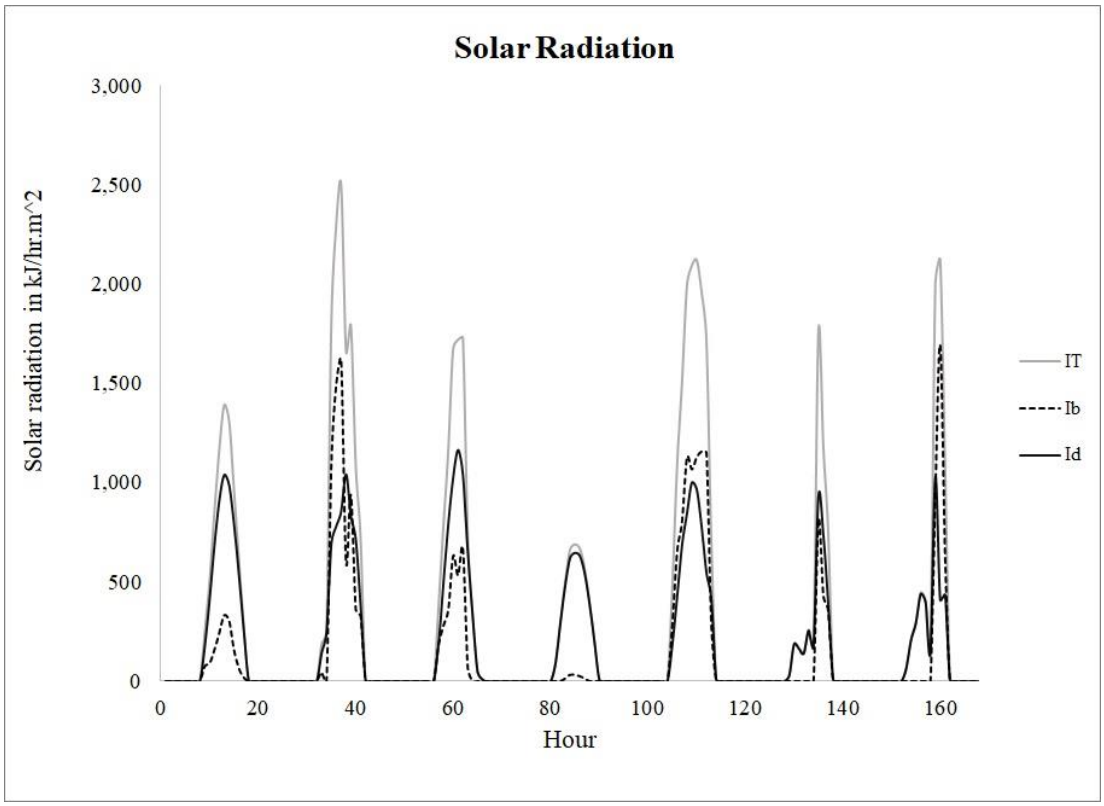

(a)

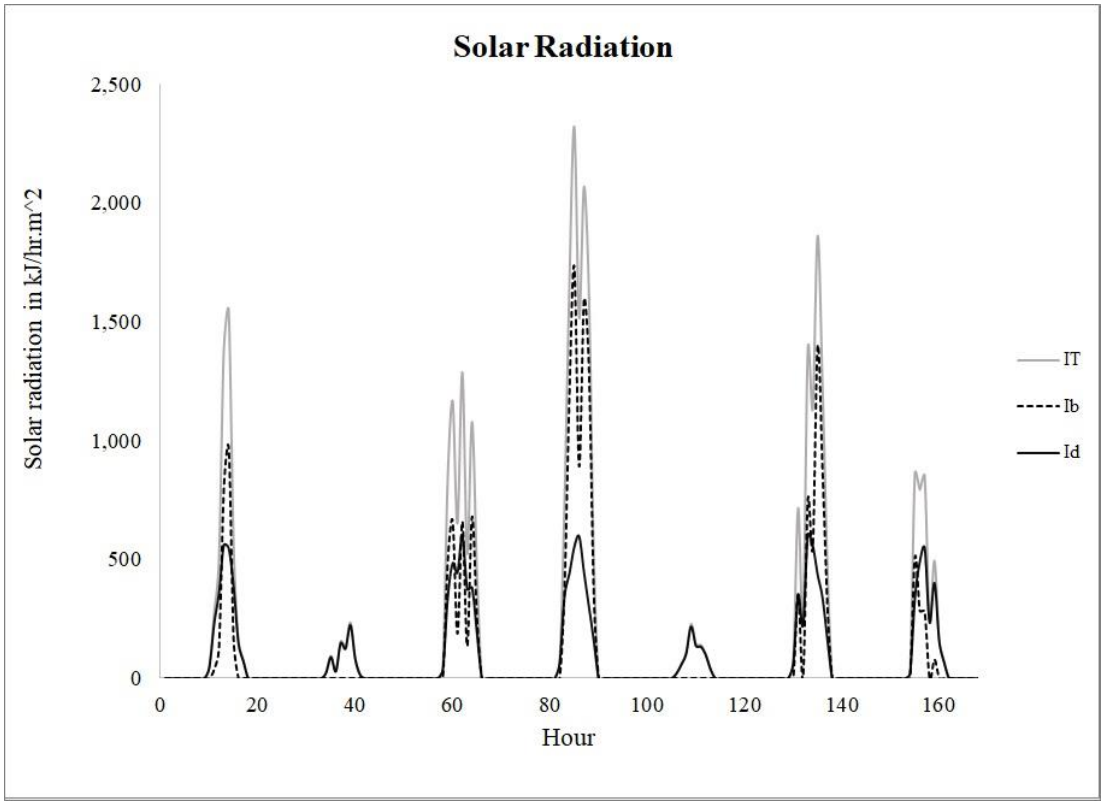

(b)

Figure 16: Total, Beam and Diffuse Solar Radiations for the First Week of January a) for Nicosia b) for London

In London, relatively less solar radiation is available. For second and fifth days of the week, very little radiation, mostly diffuse radiation, strikes the collector's apertures.

Figure 17 show useful energy gain for the CPC and flat plate collector for two cities. In January, less beam radiation is available and CPC delivers more useful solar energy compared with FPC. In Nicosia about a maximum of 2700kJ/h is collected by CPC while flat plate collector provides about 2200kJ/h in the best case. In London, maximum useful solar heat gain obtained by CPC and flat plate collector are about 2400kJ/h and 2000kJ/h, respectively. It means CPC can collect more diffuse radiation. This is the case for both cities.

Cumulative useful solar energy gains of two collectors are displayed and compared in Figure 18. Higher total useful solar energy gains at the end of the week, in case of using CPC, are clear by comparison. Cumulative useful solar energy gain of the CPC at the end of the first week of January is about 39000kJ and for flat plate collector, this value is approximately 24000kJ. For London, cumulative useful solar energy gain of the CPC and the flat plat collector are approximately 20000kJ and 10000kJ respectively, by the end of the first week of January. The gap in London is more significant.

Figure 19 show auxiliary power rates for CPC and flat plate collector, along with corresponding average values. It can be seen that blue average line is slightly above the orange one. In Nicosia, the average auxiliary power requirement for a solar water heating system with CPC is about 780kJ/h, while using a flat plat collector increase this value to about 880kJ/h. In London, the average auxiliary power requirement for CPC is slightly less than 1000kJ/h and for flat plate collector is 1060kJ/h.

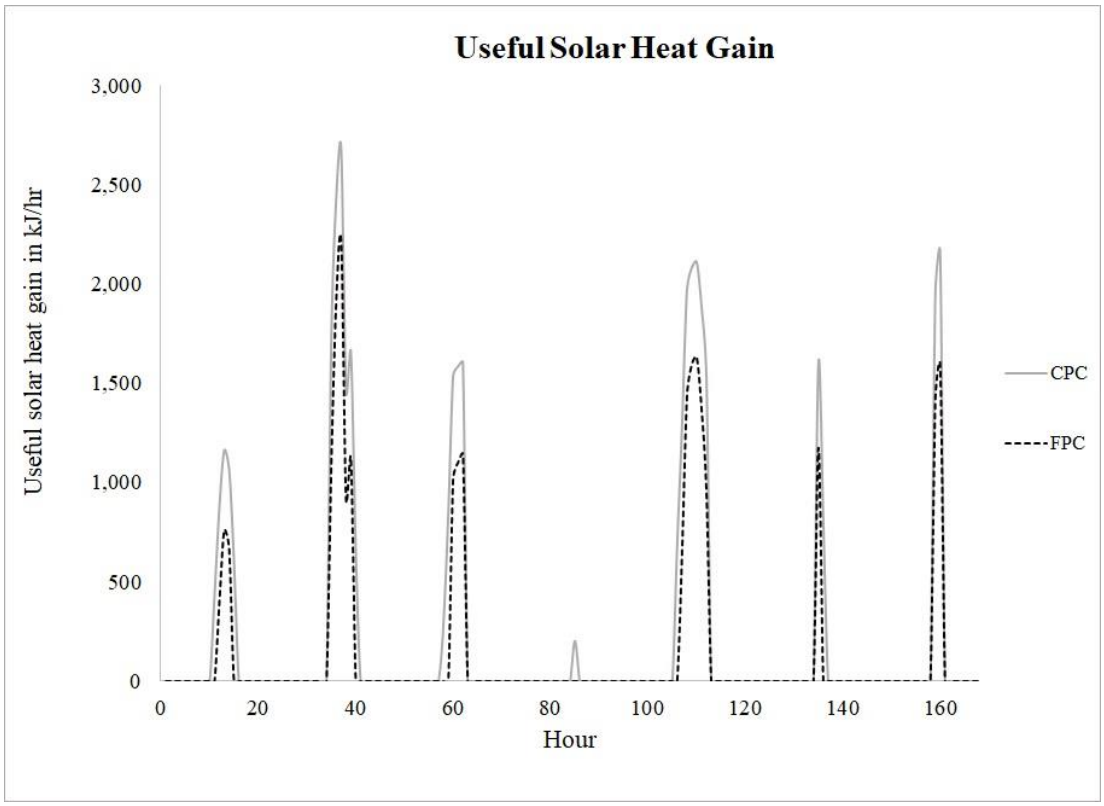

(a)

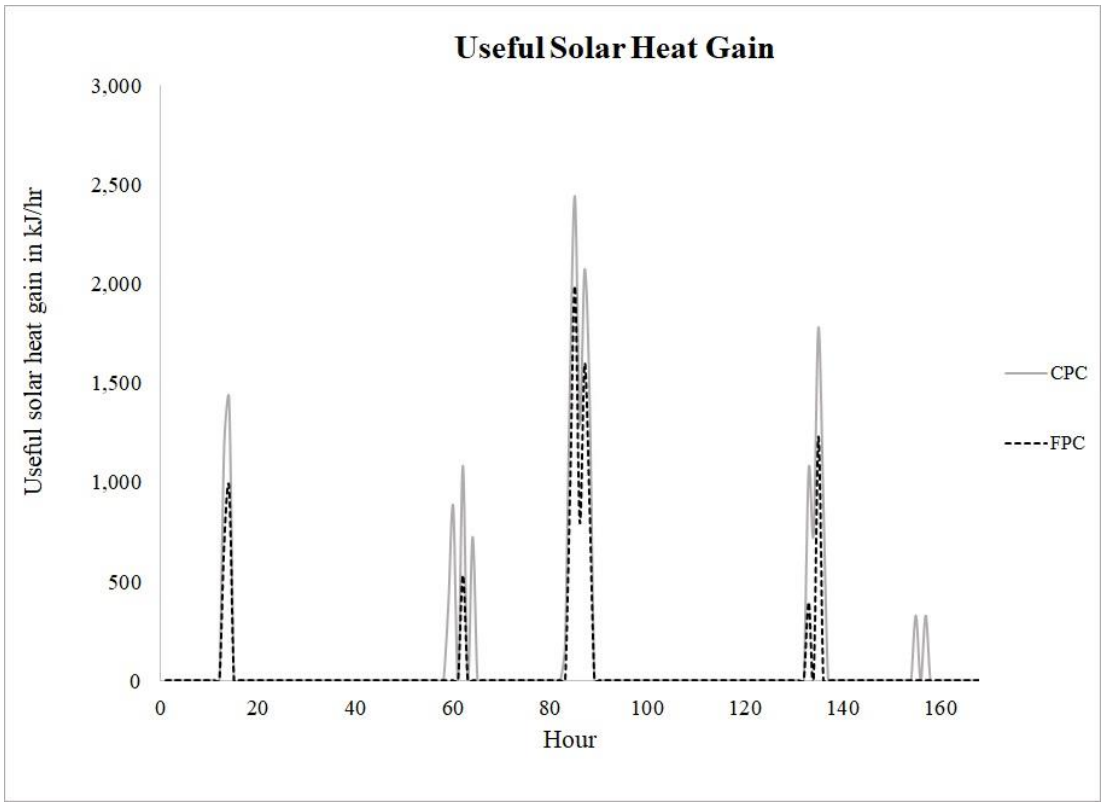

(b)

Figure 17: Useful Solar Heat Gains for the First Week of January a) for Nicosia b) for London

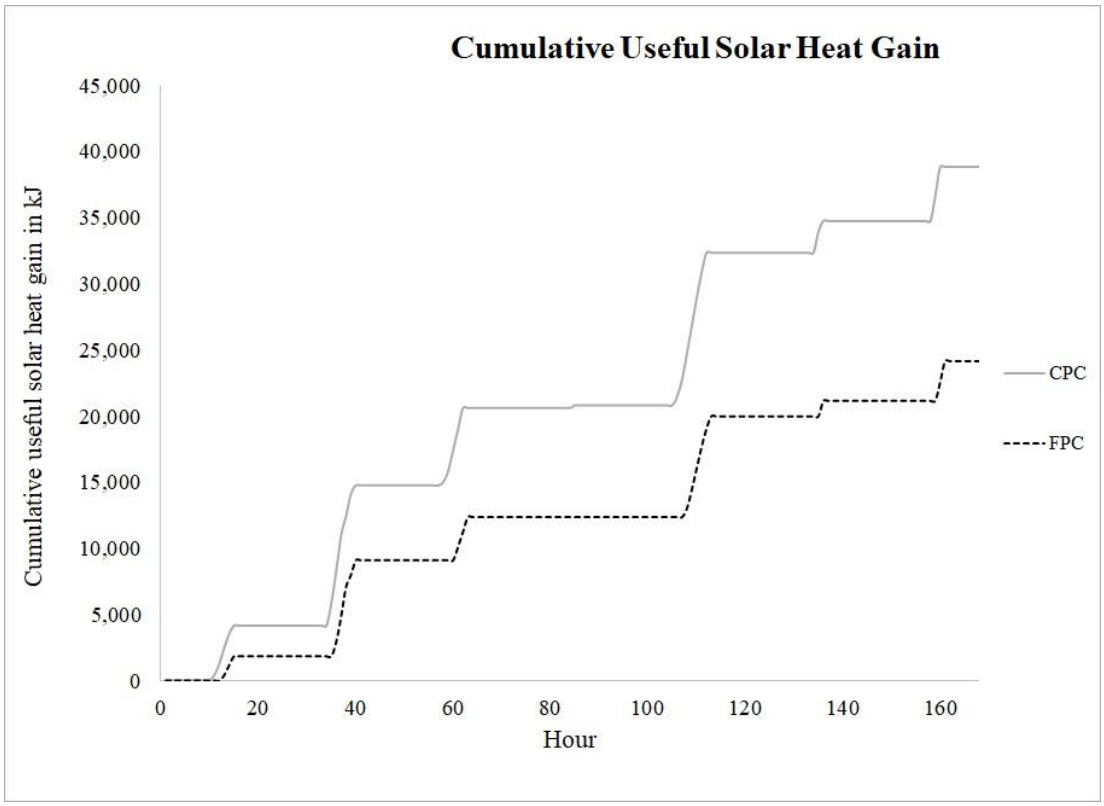

(a)

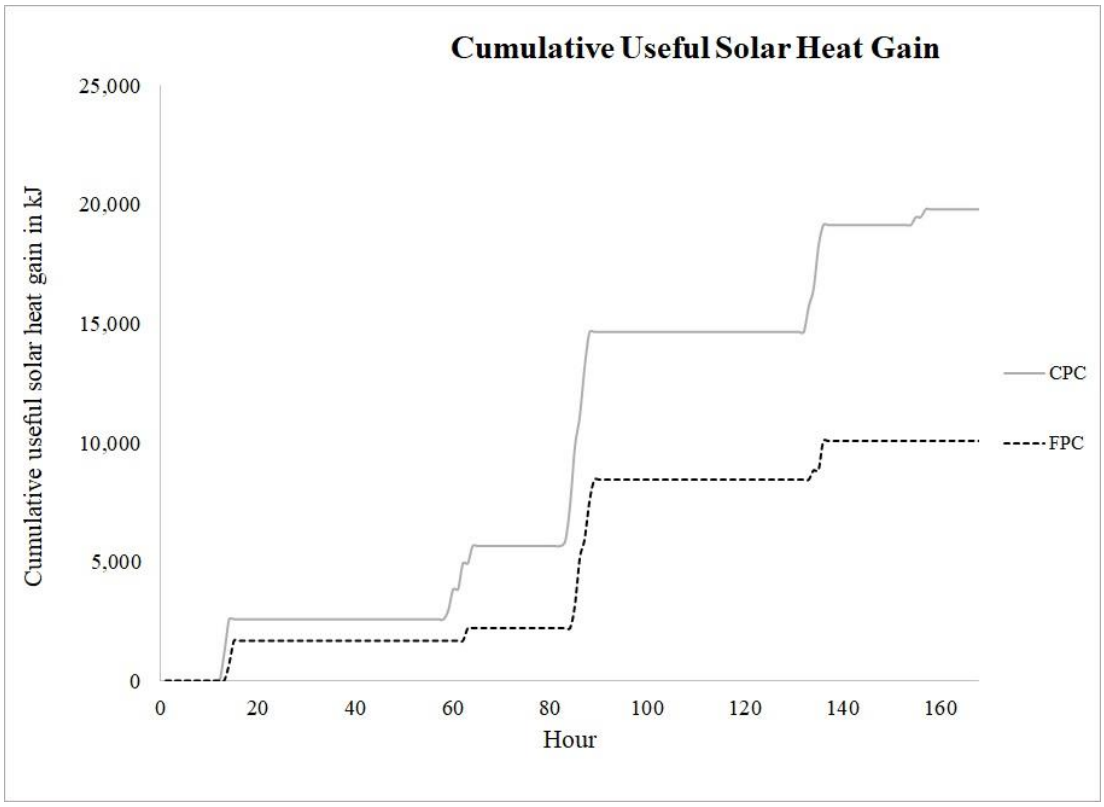

(b)

Figure 18: Cumulative Useful Solar Heat Gains for the First Week of January a) for Nicosia b) for London

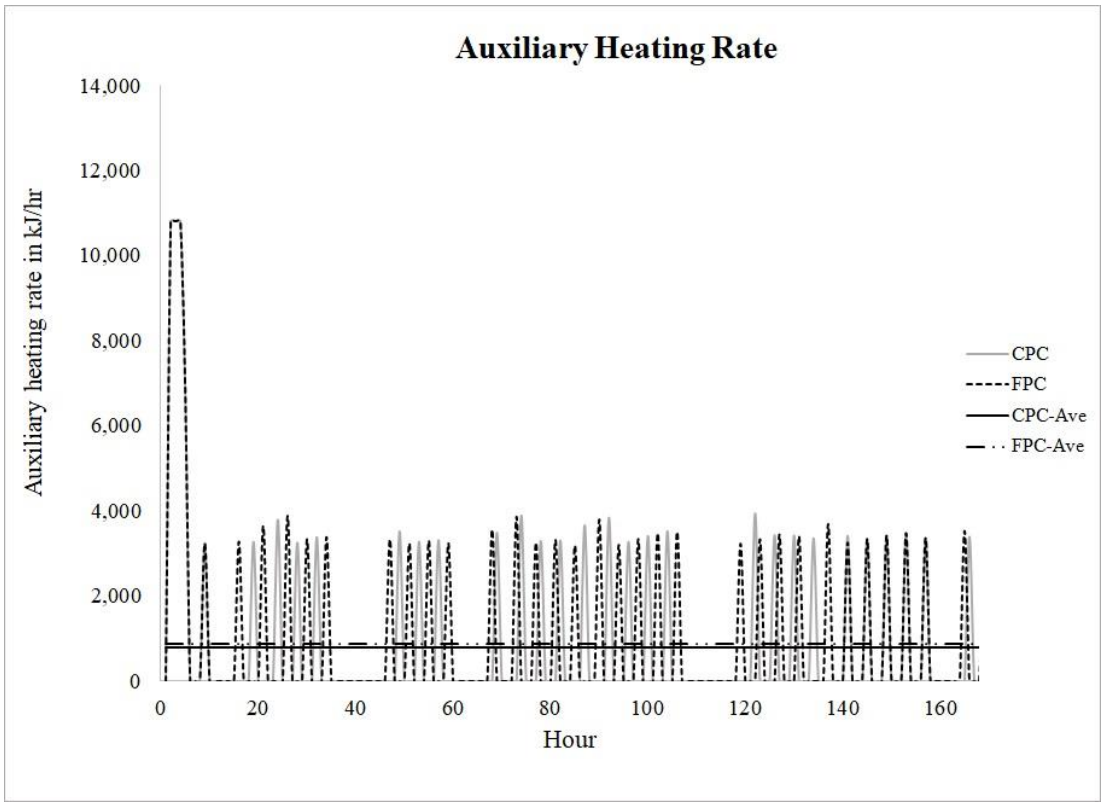

(a)

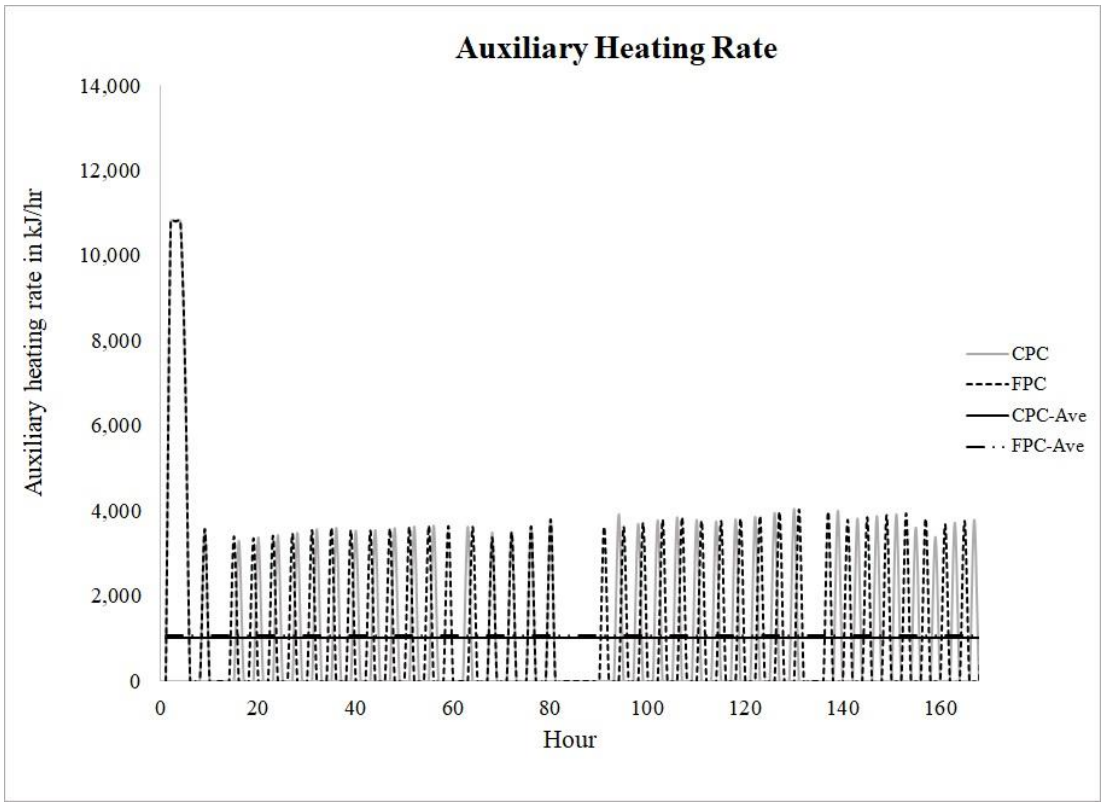

(b)

Figure 19: Auxiliary Heating Rates and Their Corresponding Averages for the First Week of January a) for Nicosia b) for London

This results means that more auxiliary power is required in the case of using a flat plate collector. This is because of the fact that CPC collects more useful energy from the sun, as shown in Figure 17, and thus less auxiliary power is needed for heating the water.

Cumulative required auxiliary energies for two collectors are displayed in Figure 20. In Nicosia, for flat plate collector, cumulative required auxiliary energy at the end of the first week of January is about 132000kJ, while in case of using a flat plate collector, this values will increase to 149000kJ. For London, cumulative required auxiliary energy for CPC and flat plate collector are approximately168000kJ and 180000kJ, respectively. In other words, in case of using a flat plate collector, more energy should be purchased. However, it should be reminded that these values are not realistic, because, as it was mentioned earlier, in this simulation it is assumed that the heater is heating the tank 24 hours a day, while this is not the case in real practice. So, smaller values for cumulative required auxiliary energies are expected in real setup. Because either the solar collector is used to provide space heating or domestic hot water, there will be a daily profile for energy demand and for some hours of the day, no heating is required. As a result, real cumulative auxiliary power requirements would be relatively lower.

Collector inlet and outlet temperatures are shown in Figure 21. It is seen that higher outlet temperatures are achieved when CPC is used. This is the consequence of collecting more useful solar energy by CPC, as shown in Figure 17. Collector inlet temperature is equal to the tank temperature essentially, since heat losses in the pipe work from the tank to the collector have been neglected.

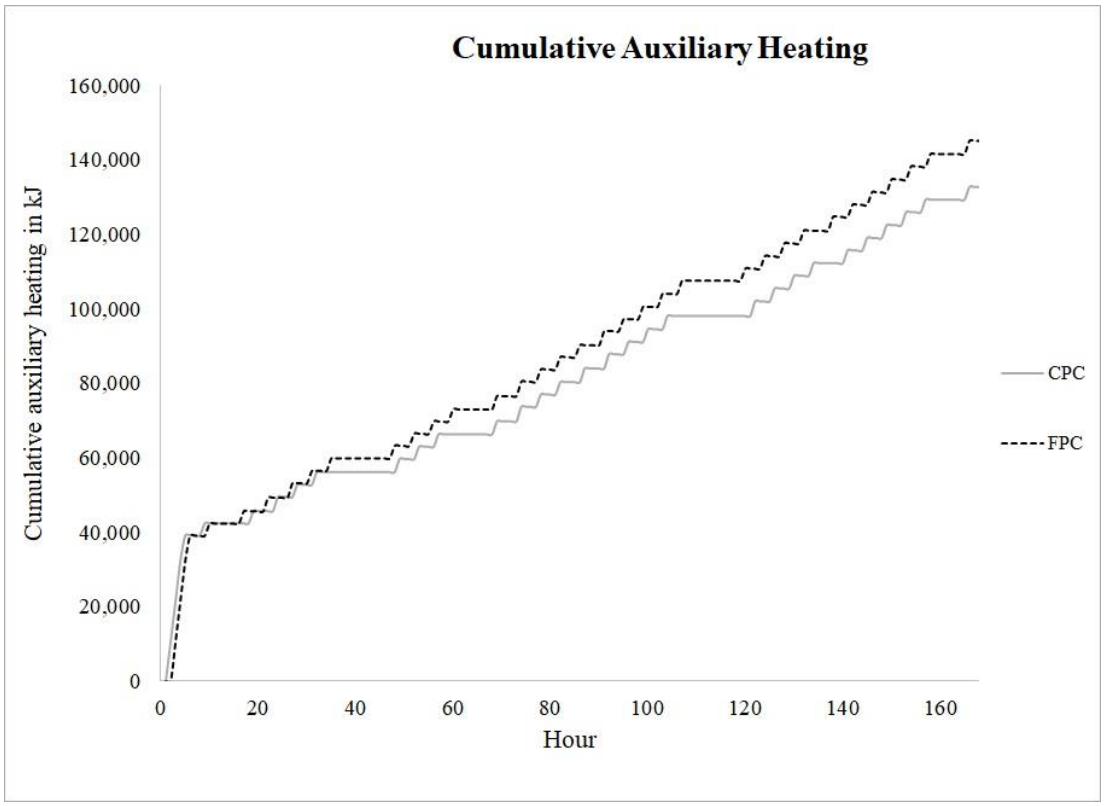

(a)

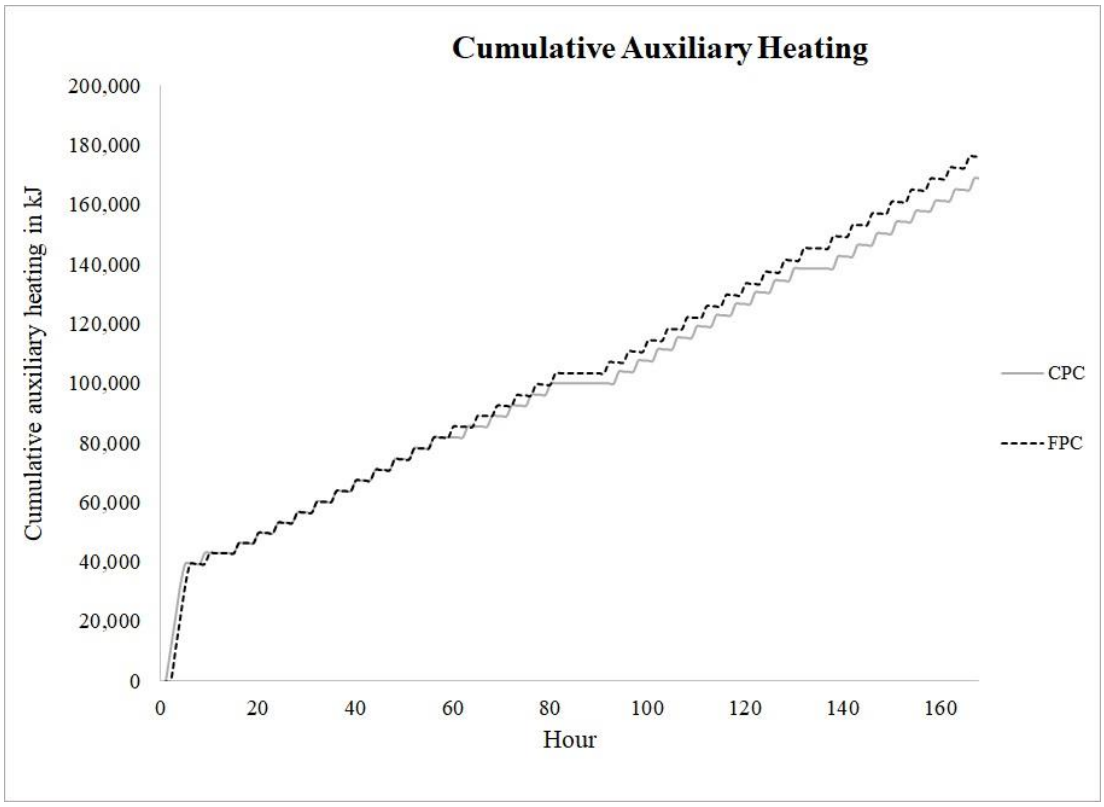

(b)

Figure 20: Cumulative Auxiliary Heating for The First Week of January a) for Nicosia b) for London

In Nicosia, in fourth day of the week, as Figure 16 shows, most of the radiation is diffuse radiation. In this day, the maximum outlet temperature of CPC is 69^{o}C, while for flat plat collector is 46^{o}C. This result is confirmed for London as well. According to Figure 16, in second and fifth day of the week, most of the radiation is diffuse radiation. Figure 21 shows that the gap between CPC and flat plate collector outlet temperatures reaches its highest value in these two days, with minimal beam radiations. Therefore, it may be concluded that in situations with limited beam radiation, utilizing CPC is more advantageous.

In Figure 22 tank temperatures for two collectors are shown. There is no stratification in this modeling. Thus, all layers of the tank have same temperature. As it was mentioned in the previous paragraphs, tank temperature is the same as the collector inlet temperature. In reality, always some degree of stratification is present in the storage tank. So, the upper layers of water have higher temperatures, and layers with lower temperature are driven to the bottom. As a result, collector inlet temperature would be equal to the bottom temperature of the tank. Top layers with higher temperatures would be derived to the load.

It is seen, in both cases of CPC and flat plate collector, tank temperatures fluctuate about 60^{o}C. This is because a heating element has been used in storage tank to maintain the tank temperature fixed at 60^{o}C. It should be mentioned that TRNSYS takes the initial tank temperature to be 0^{o}C, so at the early hours of the simulation significant temperature rise from 0^{o}C to 60^{o}C is observed, which consequently yields large auxiliary power consumption, because in the first hours of the simulation sun radiation is not available and all the required energy must be supplied by the auxiliary source.

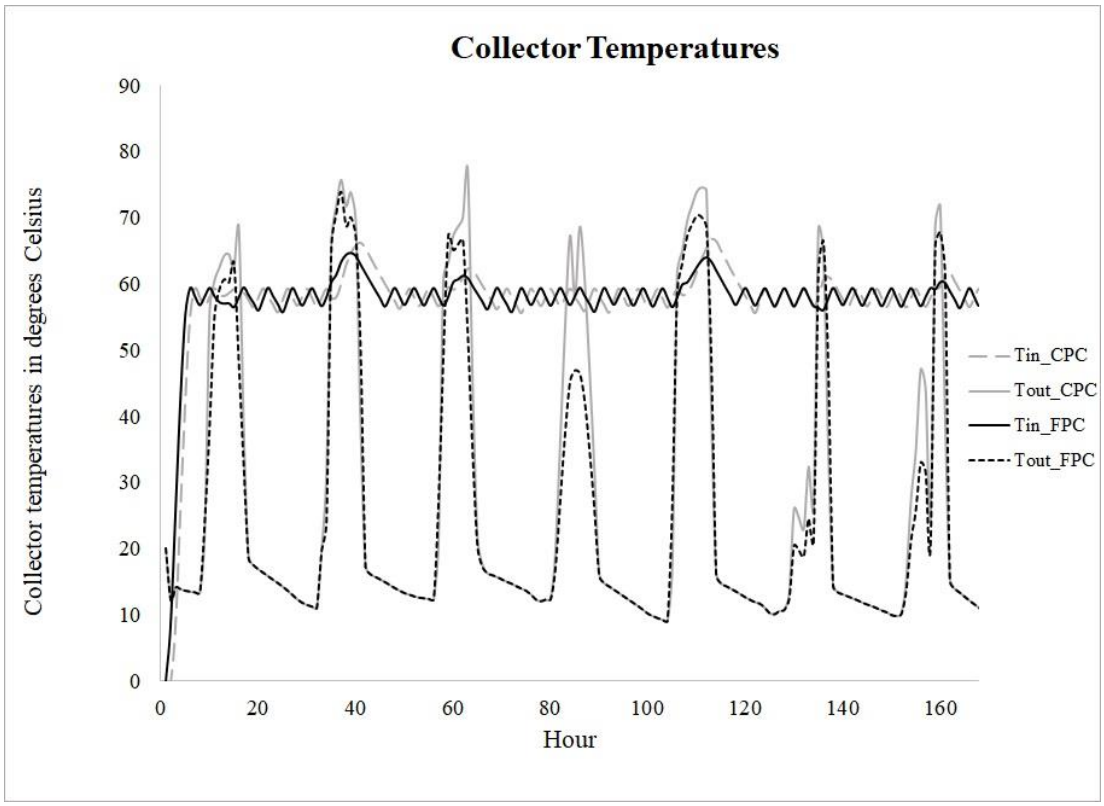

(a)

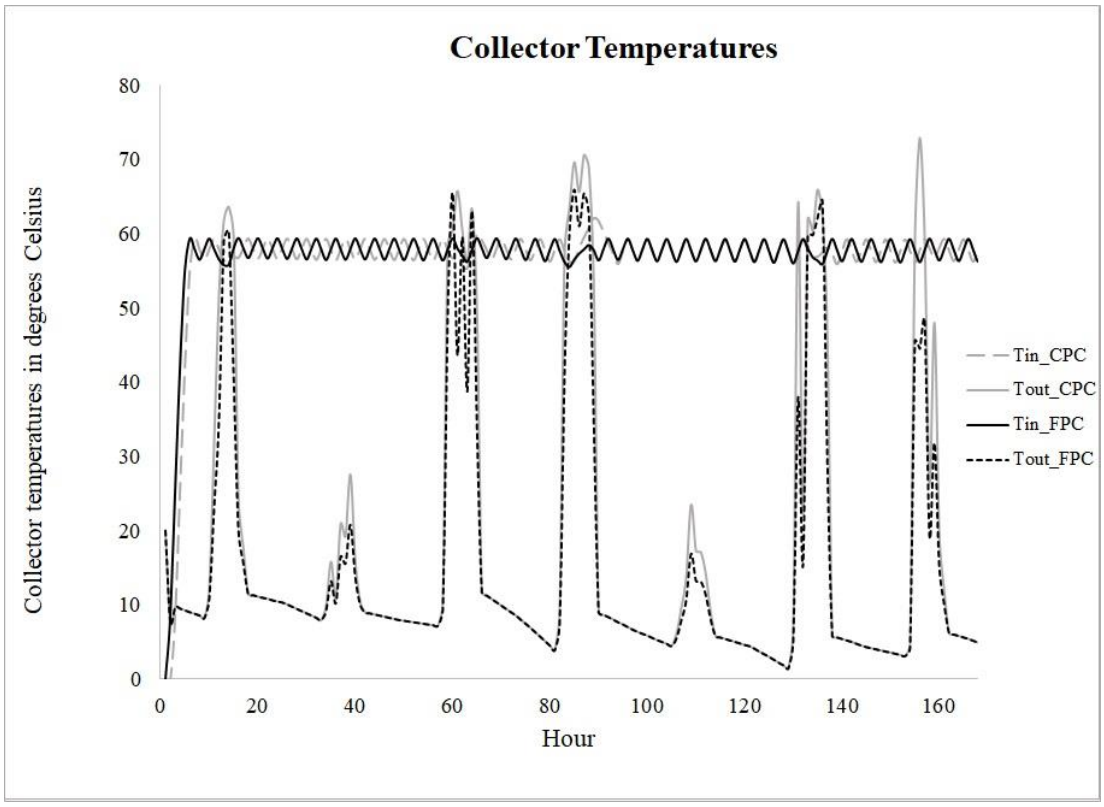

(b)

Figure 21: Collector Inlet and Outlet Temperatures for the First Week of January a) for Nicosia b) for London

However, this is not what exactly happens in real practice, thus, this huge amount of auxiliary power consumption is not realistic and care should be practiced when the auxiliary power values are reviewed and interpreted.

the dead band temperature deference of 5^{o}C allows the tank temperature to fall below the set point no more than 5^{o}C. Deviations from this set point temperature during sun radiation hours are more evident. There are some temperature peaks, corresponding to sun radiation periods in each day of the week. In these periods, tank temperature may exceed the set point temperature considerably and forms a high peak. It's seen that, in both cities, higher peaks are formed in tank temperature graphs in a solar water heating system with a CPC, meaning that higher values for tank temperatures are achieved when a CPC is used, due to higher useful solar energy collection of these collectors. Higher tank temperatures consequently mean less auxiliary power requirement, which ultimately cuts energy cost of heating purposes.

According to Figure 23, CPC achieves higher daily efficiencies compared with flat plate collector, which is directly the outcome of higher useful solar energy collection of CPC, as it's clear from Figure 17. For Nicosia, daily efficiencies of CPC are around 50%, while for flat plat collector relatively lower values are obtained, around 40%. Similarly, in London, while daily efficiencies of CPC are mostly between 40-50%, flat plat collector daily efficiencies are around 30%.

It is observed that in Nicosia, in the fourth day, CPC delivers some efficiency, while flat plate collector efficiency is almost zero. Figure 16 implies, in the fourth day of the week, almost there is no beam radiation and most of the solar radiation reaching the collector surface is diffuse radiation.

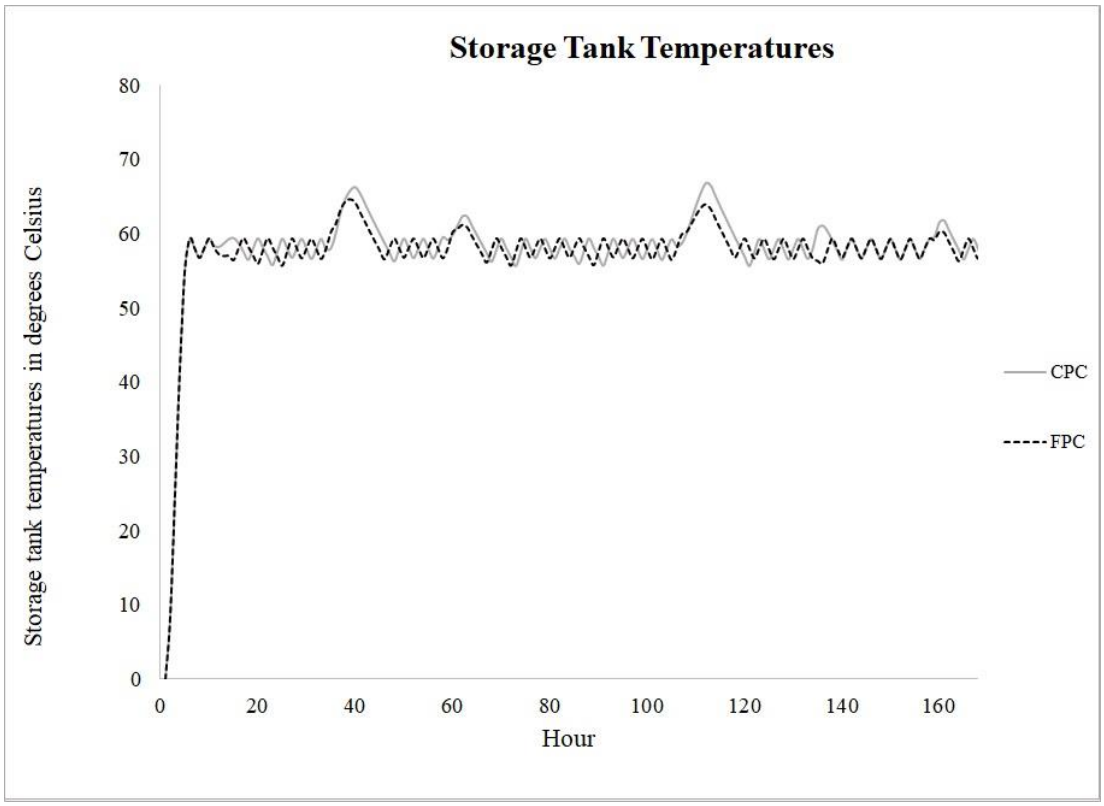

(a)

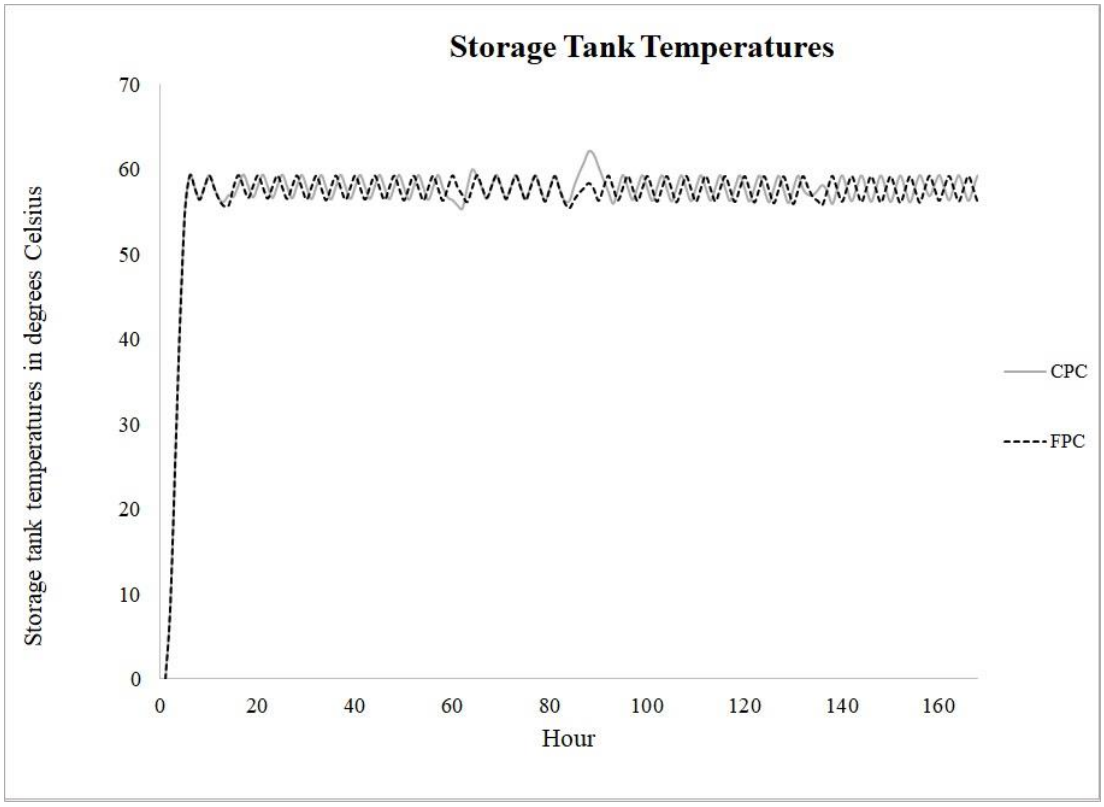

(b)

Figure 22: Tank Temperatures for the First Week of January a) for Nicosia b) for London

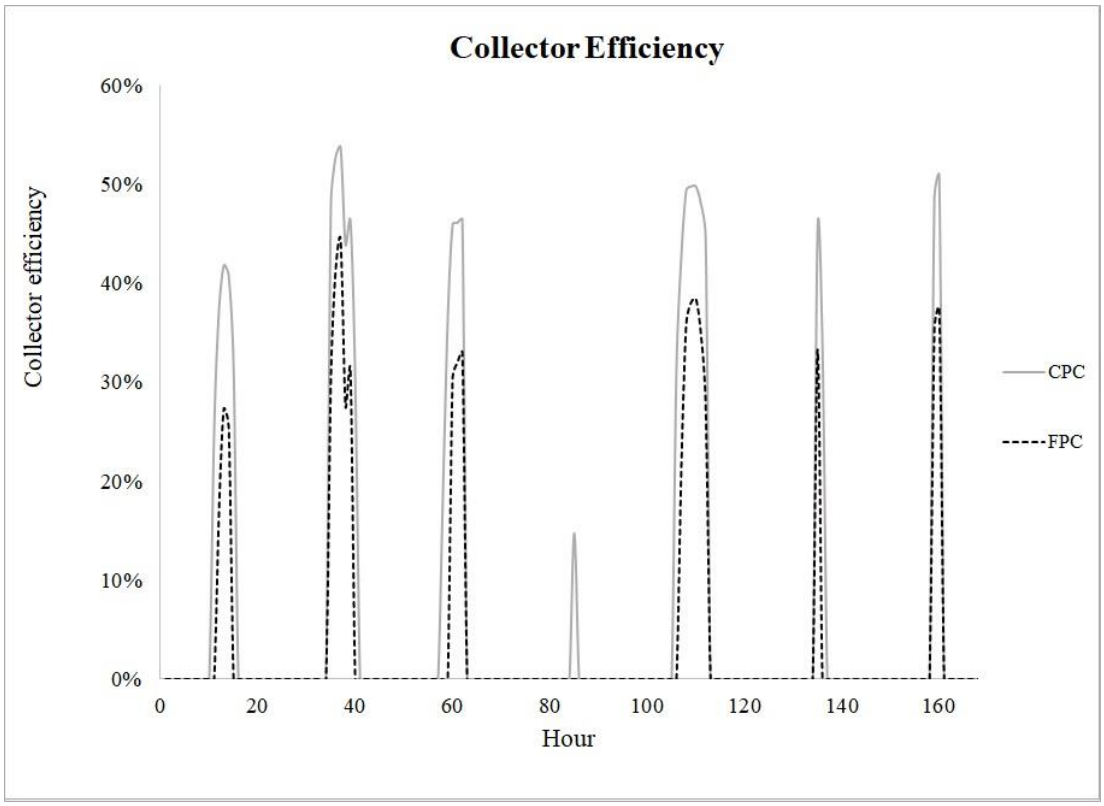

(a)

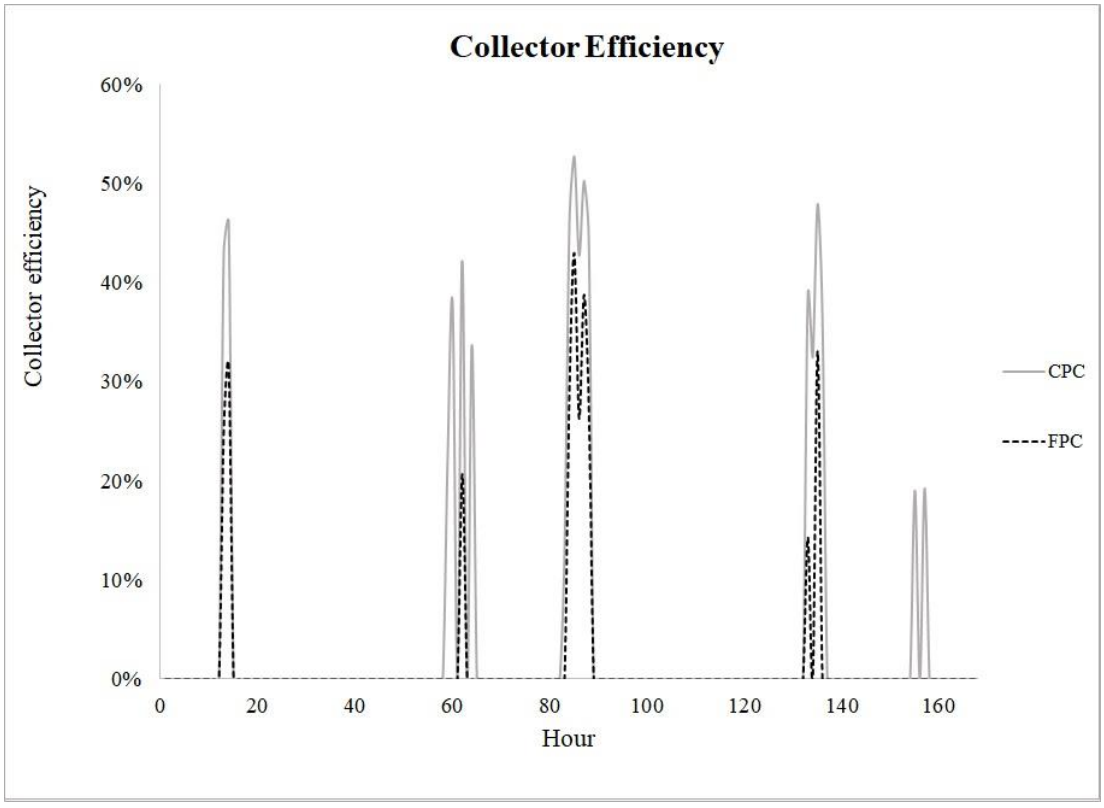

(b)

Figure 23: Collector Daily Efficiencies for the First Week of January a) for Nicosia b) for London

Table 5: Weekly Results for Nicosia for the First Week of January

Collector	Useful solar energy gain [kJ]	Required auxiliary energy [kJ]	Collector efficiency [-]
CPC	38,880	132,514	%34
Flat Plate Collector	24,179	148,530	%21

Table 6: Weekly Results for London for the First Week of January

Collector	Useful solar energy gain [kJ]	Required auxiliary energy [kJ]	Collector efficiency [-]
CPC	19,792	168,511	%30
Flat Plate Collector	10,059	179,888	%15

Therefore, CPC seems to be more efficient in collecting diffuse radiation compared with flat plate collector.

In short, in both cities, CPC collects more useful solar heat gain and provides higher efficiencies, so less auxiliary power is required. Higher useful solar energy gains result in higher collector outlet and storage tank temperatures for solar water heating systems using CPC.

Table 5 compares weekly useful solar energy gains, required auxiliary energy and collector efficiencies of CPC and flat plate collector, for Nicosia for the first week of January. Table 6 provides similar comparison for the city of London.

In Nicosia, if flat plate collector is replaced by CPC, weekly useful solar energy gain increases %61 from 24,179 kJ to 38,880 kJ which cuts required auxiliary energy %11 from 148,530 kJ to 132,514 kJ.

This means employing a CPC in a solar water heating system, instead of a typical flat plate collector, could save %11 of weekly auxiliary energy cost.

In London, although useful energy gains for both collectors are much lower compared with that of Nicosia, still CPC performance is much better. Using a CPC could increase weekly useful solar energy gain %97 from 10,059 kJ to 19,792 kJ. This reduces auxiliary power consumption by %6 from 179,888 kJ to 168,511 kJ. Therefore, also in cloudy weathers, CPC can collect more useful solar energy and reduce weekly auxiliary power requirement.

Chapter 6

CONCLUSION

The aim of this research was to simulate a domestic solar water heating system with TRNSYS for two different cities, Nicosia with abundant available solar radiation, and London with cloudy rainy weather. The simulation was carried out with two different solar collectors, one a typical flat plate collector and the other, a CPC. The performances of two collectors were compared for a period of one week.

The simulation indicates that utilizing a CPC could increase the weekly useful solar energy gain by %61 from 24,179 kJ to 38,880 kJ in Nicosia and by %97 from 10,059 kJ to 19,792 kJ in London. Consequently, collector efficiency increases from %21 to %34 in Nicosia and from %15 to %30 in London. These improvements in solar heat collection result in higher collector outlet temperatures and ultimately higher tank temperatures.

It was aimed to maintain the tank temperature at 60^{o}C 24 hours a day, throughout the week. Higher collector outlet and tank temperatures mean less auxiliary power is needed to keep the tank temperature fixed at the desired set point temperature. Weekly auxiliary power requirements for the solar water heating system decrease from 148,530 kJ to 132,514 kJ by %11 in Nicosia and from 179,888 kJ to 168,511 kJ by %6 in London.

Reduction in the auxiliary power requirement of a solar system means cutting energy costs. Thus, it could be concluded that in Nicosia, using a CPC could decrease weekly power cost by %11 in the first week of January. Similarly, %6 of weekly energy cost for this period could be saved in London.

In Northern Cyprus, crude oil is imported and burned in power plants to generate electricity. This results in high electricity rates in the country. Electricity is then used for heating water in residences. As a result, %11 reduction in weekly power requirement of residential domestic hot water applications could save substantial amount of energy and capital in a long run. This, in turn, in a bigger scale, is beneficial for the country both economically and environmentally, since less power consumption in a bigger scale means less power generation in power plants, and thus, less CO_2 emissions to the atmosphere.

Same arguments are also valid in the case of London. Using a CPC, instead of a typical flat plate collector, could decrease auxiliary power requirement of the water heating system by %6 in the first week of January. Like other European cities, effective and optimized energy consumption is a main concern. Therefore, again, CPC has advantage over flat plate collector.

In summary, employing CPC technology for domestic hot water applications, both in sunny and cloudy-rainy climates, could contribute in substantial energy savings in long run. In Appendix C, in Tables 8 and 9, yearly performance of both collectors have been presented and compared for both cities. In Nicosia, which flat plate collectors are already being used, replacing them with CPC could cut the yearly auxiliary power requirements, resulting in considerable money saving.

In London with limited beam radiation, which due to the low efficiency of flat plate collectors solar energy doesn't have a high priority, utilizing CPC could promote the application of this abundant source of thermal energy. As Tables 8 and 9 show, in London, compared with Nicosia, using a CPC for solar water heating applications, instead of a flat plate collector, is more effective in increasing the useful solar heat gain. In other words, the results suggest that utilizing a CPC in locations with low levels of beam radiation might be more beneficial.

However, there are some remarks needed to be considered. For a typical commercial flat plate collector, coefficients of equation (3-36) usually are available and are obtained based on standard tests. The first coefficient is directly related to the product of the cover transmittance and the absorber absorptance, and second coefficient is proportional to collector's overall heat loss coefficient.

In this study, the parameters for two collectors have been chosen separately, meaning that they don't have identical optical and thermal properties. So, the difference in the performances of flat plate collector and CPC, to some degree, is due to their different materials and constructions.

Since the efficiency of a flat plate collector and a CPC both strongly depend on their optical and thermal properties, its preferable to compare two collectors with similar physical properties. In this case, the difference in performances would be mainly because of the parabolic reflector. However, it's not possible to choose the parameters of two collectors in this simulation in a way that they possess exactly the same optical and thermal properties.

Instead, properties of two example collectors have been used. So, a carful experimental study on two collectors with similar absorbers and covers could yield more accurate results.

Moreover, the geometry and design of a CPC could affect its efficiency substantially. Obtaining an optimum design for a CPC with known thermal and optical properties to achieve maximum yearly efficiency is worth more work.

Finally, it should be mentioned that in this simulation, a CPC with a flat absorber was simulated. However, as it was discussed in section 2.5, different geometries for the absorber have been investigated, such as a U-shaped evacuated tabular collector with compound parabolic concentrator, innovative CPCs having a double sided absorber plate in the middle, a CPC with two receivers aligned horizontally and etc. Moreover, a dielectric CPC could be used in which the acceptance angle of the CPC for the same geometry is enlarged. Therefore, to obtain the most efficient CPC for water heating systems, techniques mentioned above or other measurements could also be incorporated.

Even though there are some limitations in this study as mentioned, like any other numerical study, still the results provide valuable information regarding the performance of CPC in domestic solar water heating systems and its potential advantage over flat plate collectors, which can be a subject of more extensive studies with experimental validations.

REFERENCES

[1] BP Energy Outlook 2018. https://www.bp.com/content/dam/bp/en/corporate/pdf/energy-economics/energy-outlook/bp-energy-outlook-2018.pdf.

[2] Thirugnanasambandam, M., Iniyan, S., & Goic, R. (2010). A review of solar thermal technologies. Renewable and sustainable energy reviews, 14(1), 312-322.

[3] Kalogirou, S. A. (2013). Solar energy engineering: processes and systems. Academic Press.

[4] International Energy Agency (IEA). Key World Energy Statistics, 2017.

[5] International Energy Agency (IEA). World Energy Outlook 2007. IEA/OECD, 2007.

[6] United Nations Development Program (UNDP). World Energy Assessment: Energy and The Challenge of Sustainability 2000.

[7] Parida, B., Iniyan, S., & Goic, R. (2011). A review of solar photovoltaic technologies. Renewable and sustainable energy reviews, 15(3), 1625-1636.

[8] Duffie, J. A., & Beckman, W. A. (2013). Solar engineering of thermal processes. John Wiley & Sons.

[9] Solar Heat for Large Buildings. SOLARGE. http://www.solarge.org/uploads/media/SOLARGE_Best_Practice_Catalogue_en.pdf.

[10] Florides, G. A., Tassou, S. A., Kalogirou, S. A., & Wrobel, L. C. (2002). Review of solar and low energy cooling technologies for buildings. Renewable and Sustainable Energy Reviews, 6(6), 557-572.

[11] Kazmerski, L. L. (1997). Photovoltaics: A review of cell and module technologies. Renewable and sustainable energy reviews, 1(1-2), 71-170.

[12] Kalogirou, S. A. (2004). Solar thermal collectors and applications. Progress in energy and combustion science, 30(3), 231-295.

[13] Schweiger, H., Mendes, J. F., Benz, N., Hennecke, K., Prieto, G., Cusí, M., & Gonçalves, H. (2000, June). The potential of solar heat in industrial processes. A state of the art review for Spain and Portugal. EuroSun.

[14] Kalogirou, S. (2003). The potential of solar industrial process heat applications. Applied Energy, 76(4), 337-361.

[15] Rommel, M., & Weiss, W. (2005). Medium temperature collectors, state of the art within task 33/IV subtask C. SHaCECotIEA (IEA),(Ed.).

[16] Jradi, M., & Riffat, S. (2012). Medium temperature concentrators for solar thermal applications. International Journal of Low-Carbon Technologies, 9(3), 214-224.

[17] Tripanagnostopoulos, Y., Souliotis, M., & Nousia, T. H. (2000). Solar collectors with colored absorbers. Solar Energy, 68(4), 343-356.

[18] Wazwaz, A., Salmi, J., Hallak, H., & Bes, R. (2002). Solar thermal performance of a nickel-pigmented aluminium oxide selective absorber. Renewable Energy, 27(2), 277-292.

[19] Orel, Z. C., Gunde, M. K., & Hutchins, M. G. (2005). Spectrally selective solar absorbers in different non-black colours. Solar Energy Materials and Solar Cells, 85(1), 41-50.

[20] Konttinen, P., Lund, P. D., & Kilpi, R. J. (2003). Mechanically manufactured selective solar absorber surfaces. Solar Energy Materials and Solar Cells, 79(3), 273-283.

[21] Benz, N., Hasler, W., Hetfleish, J., Tratzky, S., & Klein, B. (1998). Flat-plate solar collector with glass TI. In Proceedings of Eurosun (Vol. 98).

[22] Minano, J. C., Benitez, P., Gonzalez, J. C., Falicoff, W., & Caulfield, H. J. (2003). U.S. Patent No. 6,639,733. Washington, DC: U.S. Patent and Trademark Office.

[23] Winston, R. (1974). Principles of solar concentrators of a novel design. Solar Energy, 16(2), 89-95.

[24] Sun, J., & Shi, M. (2010, March). Experimental study on a concentrating solar photovoltaic/thermal system. In Power and Energy Engineering Conference (APPEEC), 2010 Asia-Pacific(pp. 1-4). IEEE.

[25] Bahaidarah, H. M., Tanweer, B., Gandhidasan, P., Ibrahim, N., & Rehman, S. (2014). Experimental and numerical study on non-concentrating and symmetric unglazed compound parabolic photovoltaic concentration systems. Applied Energy, 136, 527-536.

[26] Mallick, T. K., Eames, P. C., & Norton, B. (2006). Non-concentrating and asymmetric compound parabolic concentrating building façade integrated photovoltaics: an experimental comparison. Solar Energy, 80(7), 834-849.

[27] Arashi, H., Naito, H., Yugami, H., & Oka, T. (1997). Highly concentrated solar energy transmission through an optical fiber coupled with CPC. In Energy Conversion [28] Engineering Conference, 1997. IECEC-97., Proceedings of the 32nd Intersociety (Vol. 3, pp. 1871-1876). IEEE.

[28] Nakamaru, F., Matsumoto, Y., & Nakazono, A. (2002). Novel high-efficiency concentrator for optical fiber communication. IEEE Photonics Technology Letters, 14(7), 953-955.

[29] Pereira, M. C. (1986). Design and performance of a novel non-evacuated 1.2 x CPC type concentrator. In Intersol Eighty Five (pp. 1199-1204).

[30] Tian, M., Su, Y., Zheng, H., Pei, G., Li, G., & Riffat, S. (2018). A review on the recent research progress in the compound parabolic concentrator (CPC) for solar energy applications. Renewable and Sustainable Energy Reviews, 82, 1272-1296.

[31] Kim, Y., Han, G., & Seo, T. (2008). An evaluation on thermal performance of CPC solar collector. International Communications in Heat and Mass Transfer, 35(4), 446-457.

[32] Khalifa, A. J. N., & Al-Mutawalli, S. S. (1998). Effect of two-axis sun tracking on the performance of compound parabolic concentrators. Energy Conversion and Management, 39(10), 1073-1079.

[33] Rabl, A. (1976). Optical and thermal properties of compound parabolic concentrators. Solar energy, 18(6), 497-511.

[34] Tchinda, R., & Ngos, N. (2006). A theoretical evaluation of the thermal performance of CPC with flat one-sided absorber. International Communications in Heat and Mass Transfer, 33(6), 709-718.

[35] Rönnelid, M., Perers, B., & Karlsson, B. (1996). Construction and testing of a large-area CPC-collector and comparison with a flat plate collector. Solar energy, 57(3), 177-184.

[36] Zambolin, E., & Del Col, D. (2010). Experimental analysis of thermal performance of flat plate and evacuated tube solar collectors in stationary standard and daily conditions. Solar Energy, 84(8), 1382-1396.

[37] Qin, L., & Furbo, S. (1998). Solar heating systems with evacuated tubular solar collector. In EuroSun'98.

[38] Winston, R., O'Gallagher, J., Muschaweck, J., Mahoney, A., & Dudley, V. (1999). Comparison of predicted and measured performance of an integrated compound parabolic concentrator (ICPC). In Proceedings of ISES Solar World Congress on CDROM, Jerusalem, Israel.

[39] Grass, C., Benz, N., Hacker, Z., & Timinger, A. (2000). Tube collector with integrated tracking parabolic concentrator. In Proceedings of the Eurosun'2000 Conference on CD-ROM, Copenhagen, Denmark (p. 327).

[40] ASHRAE, A. H. H. (2016). Systems and equipment. ASHRAE, Atlanta, GA.

[41] Gil, A., Medrano, M., Martorell, I., Lázaro, A., Dolado, P., Zalba, B., & Cabeza, L. F. (2010). State of the art on high temperature thermal energy storage for power generation. Part 1—Concepts, materials and modellization. Renewable and Sustainable Energy Reviews, 14(1), 31-55.

[42] Hale, M. (2000). Survey of thermal storage for parabolic trough power plants. NREL Report, No. NREL/SR-550-27925, 1-28.

[43] Zhao, C. Y., & Wu, Z. G. (2011). Thermal property characterization of a low melting-temperature ternary nitrate salt mixture for thermal energy storage systems. Solar Energy Materials and Solar Cells, 95(12), 3341-3346.

[44] Zhao, C. Y., Zhou, D., & Wu, Z. G. (2010, January). Heat transfer enhancement of phase change materials (PCMs) in low and high temperature thermal storage by using porous materials. In 2010 14th International Heat Transfer Conference (pp. 435-441). American Society of Mechanical Engineers.

[45] Tian, Y., & Zhao, C. Y. (2013). A review of solar collectors and thermal energy storage in solar thermal applications. Applied energy, 104, 538-553.

[46] Timinger, A., Kribus, A., Doron, P., & Ries, H. (2000). Faceted concentrators optimized for homogeneous radiation. Applied Optics, 39(7), 1152-1158.

[47] van Dijk, L., Marcus, E. P., Oostra, A. J., Schropp, R. E., & Di Vece, M. (2015). 3D-printed concentrator arrays for external light trapping on thin film solar cells. Solar Energy Materials and Solar Cells, 139, 19-26.

[48] Cooper, T., Dähler, F., Ambrosetti, G., Pedretti, A., & Steinfeld, A. (2013). Performance of compound parabolic concentrators with polygonal apertures. Solar Energy, 95, 308-318.

[49] Welford, W. T., & Winston, R. (1978). Optics of nonimaging concentrators. Light and solar energy.

[50] Baig, H., Sellami, N., Chemisana, D., Rosell, J., & Mallick, T. K. (2014). Performance analysis of a dielectric based 3D building integrated concentrating photovoltaic system. Solar Energy, 103, 525-540.

[51] Baig, H., Sarmah, N., Chemisana, D., Rosell, J., & Mallick, T. K. (2014). Enhancing performance of a linear dielectric based concentrating photovoltaic system using a reflective film along the edge. Energy, 73, 177-191.

[52] Walze, G., Nitz, P., Ell, J., Georg, A., Gombert, A., & Hossfeld, W. (2005). Combination of microstructures and optically functional coatings for solar control glazing. Solar energy materials and solar cells, 89(2-3), 233-248.

[53] Arnaoutakis, G. E., Marques-Hueso, J., Ivaturi, A., Fischer, S., Goldschmidt, J. C., Krämer, K. W., & Richards, B. S. (2015). Enhanced energy conversion of up-conversion solar cells by the integration of compound parabolic concentrating optics. Solar energy materials and solar cells, 140, 217-223.

[54] Ortiz-Rivera, E. I., & Feliciano-Cruz, L. I. (2009, September). Performance evaluation and simulation of a solar thermal power plant. In Energy Conversion Congress and Exposition, 2009. ECCE 2009. IEEE (pp. 337-344). IEEE.

[55] Al-Ghasem, A., Tashtoush, G., & Aladeemy, M. (2013, October). Experimental study of tracking 2-D Compound Parabolic Concentrator (CPC) with flat plate absorber. In Renewable Energy Research and Applications (ICRERA), 2013 International Conference on (pp. 779-782). IEEE.

[56] Mishra, R. K., Garg, V., & Tiwari, G. N. (2017). Energy matrices of U-shaped evacuated tubular collector (ETC) integrated with compound parabolic concentrator (CPC). Solar Energy, 153, 531-539.

[57] Ratismith, W., Inthongkhum, A., & Briggs, J. (2014). Two non-tracking solar collectors: Design criteria and performance analysis. Applied energy, 131, 201-210.

[58] Abdullahi, B., Al-Dadah, R. K., & Mouhmud, S. (2014). Optical performance of double receiver compound parabolic concentrator. Energy Procedia, 61, 2625-2628.

[59] Abdullahi, B., Al-Dadah, R. K., Mahmoud, S., & Hood, R. (2015). Optical and thermal performance of double receiver compound parabolic concentrator. Applied energy, 159, 1-10.

[60] Antonelli, M., Baccioli, A., Francesconi, M., Desideri, U., & Martorano, L. (2015). Electrical production of a small size Concentrated Solar Power plant with compound parabolic collectors. Renewable Energy, 83, 1110-1118.

[61] Tiwari, D., Sherwani, A. F., Atheaya, D., & Arora, A. (2017). Energy and exergy analysis of solar driven recuperated organic Rankine cycle using glazed reverse absorber conventional compound parabolic concentrator (GRACCPC) system. Solar Energy, 155, 1431-1442.

[62] Trnsys, A. (2000). Transient System Simulation Program. University of Wisconsin.

APPENDICES

Appendix A: MATLAB Code

In this appendix, a MATLAB code based on TRNSYS version 16.01.0003 formulation, presented in section 3.2.1, is provided to model and simulate a CPC. The code calculates the annual useful solar heat gain of a CPC and was run and tested for Nicosia, which the results were in agreement with TRNSYS within 1.2% error.

The same data Type74 (CPC collector) in TRNSYS reads from Type109-TMY2, the MATLAB code also reads from external files containing the outputs of Type109-TMY2. This was done in the code section titled "%Reading data from TRNSYS - Type109-TMY2". In the code section titled "%TRNSYS Input parameters", the parameters of CPC are set in a similar manner with TRNSYS. All power units are kJ/hr. The code calculates the useful solar heat gain of the CPC for each 8760 hour of a year and add them together to obtain the annual useful solar heat gain. It is possible to run the code in two possible collector axis orientation modes, mode 1 for transverse and mode 2 for longitudinal.

```
%Cleaning the command window
clc

%Setting the tracking axis mode
Mode = input('Please enter the tracking axis mode (1 for
transverse and 2 for longitudinal): ');

%Reading data from TRNSYS - Type109-TMY2
fileID = fopen('Hour.txt','r');
formatSpec = '%f';
hr = fscanf(fileID,formatSpec);
fclose(fileID);

fileID = fopen('Gamma_s.txt','r');
formatSpec = '%f';
Gammas = fscanf(fileID,formatSpec);
fclose(fileID);

fileID = fopen('Theta_z.txt','r');
formatSpec = '%f';
Thetaz = fscanf(fileID,formatSpec);
fclose(fileID);

fileID = fopen('Theta1.txt','r');
formatSpec = '%f';
Theta = fscanf(fileID,formatSpec);
fclose(fileID);

fileID = fopen('I.txt','r');
formatSpec = '%f';
Ih = fscanf(fileID,formatSpec);
fclose(fileID);

fileID = fopen('I_d.txt','r');
formatSpec = '%f';
Id = fscanf(fileID,formatSpec);
fclose(fileID);

fileID = fopen('I_T.txt','r');
formatSpec = '%f';
IT = fscanf(fileID,formatSpec);
fclose(fileID);

fileID = fopen('T_a.txt','r');
formatSpec = '%f';
Ta = fscanf(fileID,formatSpec);
fclose(fileID);

%TRNSYS Input parameters
A_a = 2;
C_p = 4.19;
```

```
F_prime = 0.92;
U_L = 9;
Rho_R = 0.9;
Theta_c = 35;
TruncationRatio = 0.1;
Alpha = 0.87;
n_g = 1.526;
KL = 0.0026;
T_i = 20;
m_dot = 72;
Rho_g = 0.2;
Beta = 35;
Gamma = 0;

%CPC parameters
SINTC = sind(Theta_c);
SINSQ = SINTC*SINTC;
COSHAF = cosd(Theta_c);
COSSQ = COSHAF*COSHAF;
COTSQ = COSSQ/SINSQ;
SINHF1 = SINTC + 1;
XBAR1 = SINHF1/COSHAF*(-SINTC + sqrt(1 +
TruncationRatio*COTSQ));
C = (2*COSHAF*XBAR1) - (XBAR1*XBAR1*SINTC/SINHF1) + SINTC
- COSSQ;
AA = sqrt(SINHF1*SINHF1 + XBAR1*XBAR1);
BB = sqrt(2)*sqrt(SINHF1);
CC = sqrt(1 + XBAR1*XBAR1/SINHF1/SINHF1);
AFRACT = SINHF1*log((XBAR1 + AA)/(COSHAF + BB)) +
XBAR1*CC - sqrt(2)*COSHAF/sqrt(SINHF1);
ENI = 0.5*(AFRACT - (XBAR1*XBAR1 - COSSQ)/SINHF1);
RHOEFF = Rho_R^ENI;
ALF = Alpha*RHOEFF;

%Setting initial values for solar total useful heat gain
Q_u_total = 0;

for i = 1:8761
 Hour = hr(i);
 T_a = Ta(i);
 I_T = IT(i);
 I = Ih(i);
 I_d = Id(i);
 Theta1 = Theta(i);
 Theta_z = Thetaz(i);
 Gamma_s = Gammas(i);

 %Use effective incidence angle for difue and grund
reflected radiations
 Theta_d = 44.86 - 0.0716*Theta_c + 0.00512*Theta_c^2 -
0.00002798*Theta_c^3;
```

```
  %Tracking axis mode
  switch Mode
   case 1 %Transverse
    FSKY = (1/C + min(1/C,cosd(Beta)))/2;
    FGND = (max(1/C,cosd(Beta)) - cosd(Beta))/2;
    TANALF = tand(Theta_z)*cosd(Gamma - Gamma_s);
    THETAP = abs(atand(TANALF) - Beta);
   case 2 %Longitudinal
    FSKY = (1 + cosd(Beta))/(2*C);
    FGND = (1 - cosd(Beta))/(2*C);
    TANTP = sind(Theta_z)*sind(abs(Gamma -
Gamma_s))/cosd(Theta1);
    THETAP = atand(TANTP);
  end

 %Check for sun angle within acceptance of the collector
 FB = 0;
 if THETAP < Theta_c
  FB = 1;
 end

 %TALF routine for diffuse radiation
 THETA1 = Theta_d;
 THETA2 = asind(sind(THETA1)/n_g);
 R(1) = sind(THETA2 - THETA1);
 R(2) = sind(THETA2 + THETA1);
 T(1) = R(1)/cosd(THETA2 - THETA1);
 T(2) =R(2)/cosd(THETA2 + THETA1);
 RHO(1) = R(1)*R(1)/R(2)/R(2);
 RHO(2) = T(1)*T(1)/T(2)/T(2);
 TABS= exp(-KL/cosd(THETA2));
 for J=1:2
  T(J) = TABS*(1 - RHO(J))^2/(1 -
TABS*TABS*RHO(J)*RHO(J));
  R(J) = RHO(J)*(1 + TABS*T(J));
  TAU(J) = T(J);
  REF(J) = R(J);
 end
 RHOD = (REF(1) + REF(2))/2;
 TAU_ALPHAD = (TAU(1) + TAU(2))/2*ALF/(1 - (1 -
ALF)*RHOD);

 %TALF routine for beam radiation
 THETA1 =  Theta1;
 if THETA1 < 0.001
    THETA1 = 0.001;
 end
 R(1) = sind(THETA2 - THETA1);
 R(2) = sind(THETA2 + THETA1);
 T(1) = R(1)/cosd(THETA2 - THETA1);
 T(2) =R(2)/cosd(THETA2 + THETA1);
```

```
 RHO(1) = R(1)*R(1)/R(2)/R(2);
 RHO(2) = T(1)*T(1)/T(2)/T(2);
 TABS= exp(-KL/cosd(THETA2));
 for J=1:2
  T(J) = TABS*(1 - RHO(J))^2/(1 -
TABS*TABS*RHO(J)*RHO(J));
  TAU(J) = T(J);
 end
 TAU_ALPHAB = (TAU(1) + TAU(2))/2*ALF/(1 - (1 -
ALF)*RHOD);

 %TALF routine for normal radiation
 THETA1 = 0.001;
 THETA2 = asind(sind(THETA1)/n_g);
 R(1) = sind(THETA2 - THETA1);
 R(2) = sind(THETA2 + THETA1);
 T(1) = R(1)/cosd(THETA2 - THETA1);
 T(2) =R(2)/cosd(THETA2 + THETA1);
 RHO(1) = R(1)*R(1)/R(2)/R(2);
 RHO(2) = T(1)*T(1)/T(2)/T(2);
 TABS= exp(-KL/cosd(THETA2));
 for J=1:2
  T(J) = TABS*(1 - RHO(J))^2/(1 -
TABS*TABS*RHO(J)*RHO(J));
  TAU(J) = T(J);
 end
 TAU_ALPHAN = (TAU(1) + TAU(2))/2*ALF/(1 - (1 -
ALF)*RHOD);

 %Absorbed solar radiation
 XKATB = TAU_ALPHAB/TAU_ALPHAN;
 XKATB = XKATB*FB;
 XKATD = TAU_ALPHAD/TAU_ALPHAN;
 GB = I_T - I_d*(1 + cosd(Beta))/2 - Rho_g*I*(1 -
cosd(Beta))/2;
 GDT = I_d*FSKY + Rho_g*I*FGND;
 XKAT = 1;
 if (I_T == 0) | (Theta1 > 90) %Determine incidence angle
modifier
  XKAT = 0;
 else
  XKAT = (XKATB*GB + XKATD*GDT)/I_T;
 end

 %Ueful heat gain
 F_R = m_dot*C_p/(A_a*U_L)*(1 - exp(-
A_a*U_L*F_prime/(m_dot*C_p)));
 Q_u(i) = F_R*A_a*(I_T*TAU_ALPHAN*XKAT - U_L*(T_i-T_a));
 Q_u_total =  Q_u_total + Q_u(i);
 Q_u_1_total = 9.09*10^6;
 Q_u_2_total = 6.89*10^6;
```

```
end

%Printing the results
switch Mode
 case 1 %Transverse
  Error = abs(Q_u_total - Q_u_1_total)/Q_u_1_total*100;
  fprintf('The tracking axis mode is %g
(transverse).\n',Mode)
  fprintf('Q_u_total = %3.2f MJ.\n',Q_u_total/10^6)
  fprintf('TRNSYS answer = %3.2f MJ.\n',Q_u_1_total/10^6)
  fprintf('Erroe = %3.1f%%.\n',Error)
 case 2 %Longitudinal
  Error = abs(Q_u_total - Q_u_2_total)/Q_u_2_total*100;
  fprintf('The tracking axis mode is %g
(longitudinal).\n',Mode)
  fprintf('Q_u_total = %3.2f MJ.\n',Q_u_total/10^6)
  fprintf('TRNSYS answer = %3.2f MJ.\n',Q_u_2_total/10^6)
  fprintf('Erroe is %3.1f%%.\n',Error)
end
```

Appendix B: Geometrical Description and Dimensions of CPC

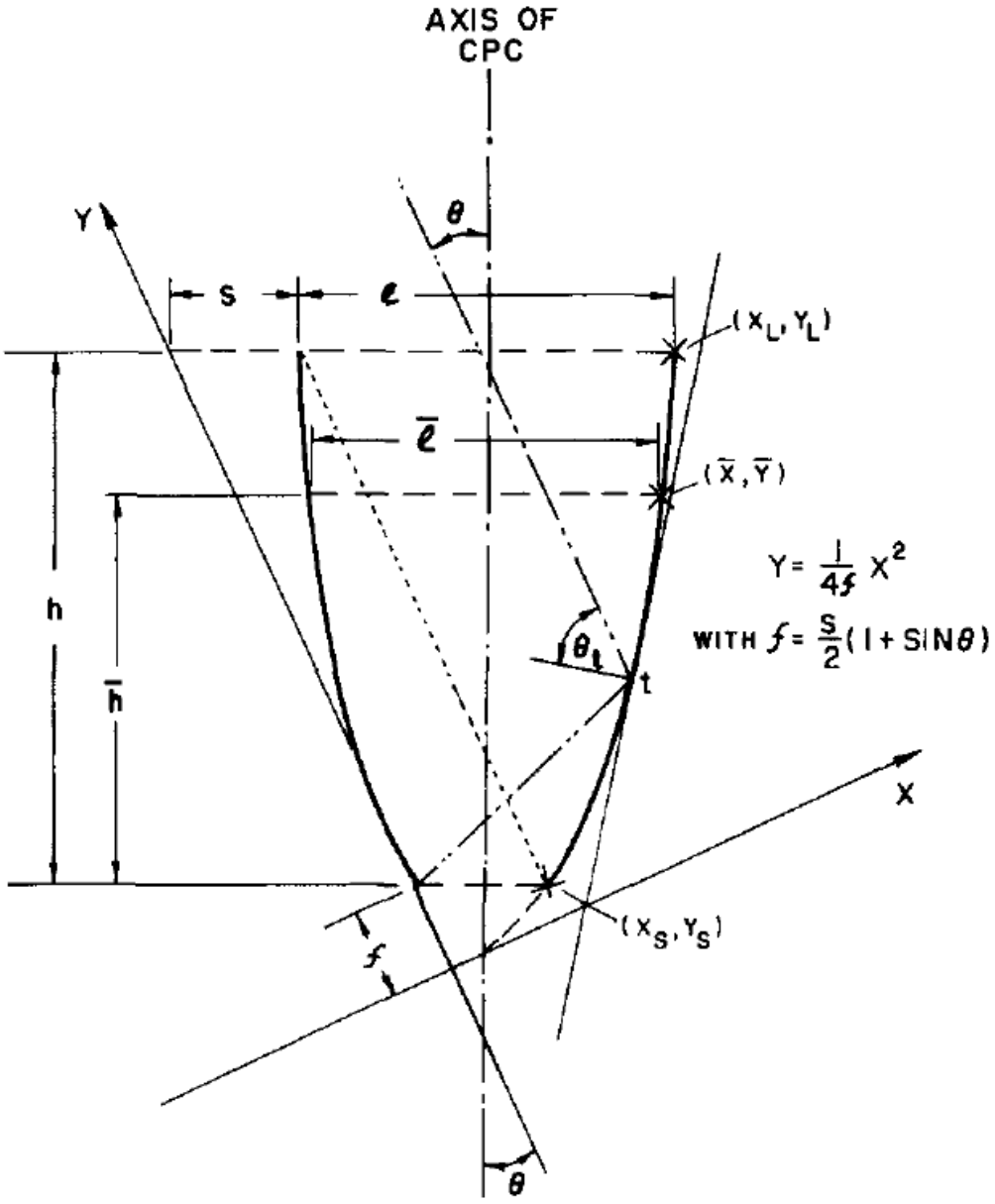

Figure 24: Detailed Geometrical Description of a CPC [33]

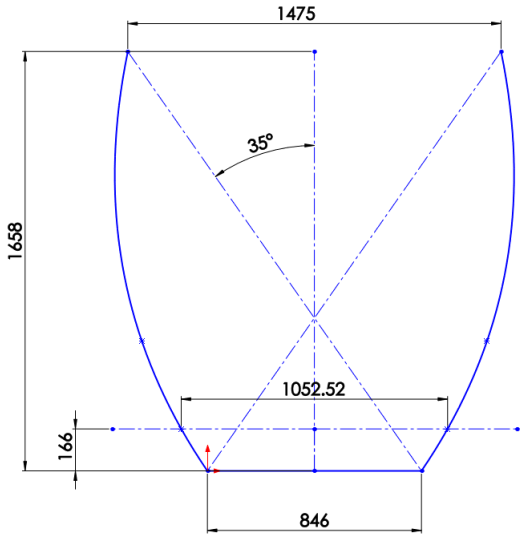

Figure 25: A Drawing of the Simulated CPC

Using the MATLAB code provided in Appendix A and parameters given in Table 2, all other parameters of the simulated CPC have been calculated and presented in Table 7. The symbols refer to Figure 13. The aperture has an area of $2m^2$ with 1m width and 2m length. Also, Figure 25 shows a drawing of the corresponding CPC.

Table 7: Dimensions of the Simulated CPC

Parameter	Symbol	Value
Aperture area	A_a	$2m^2$
Half-acceptance angle	θ_c	o
Truncation ratio	$\frac{\bar{h}}{h}$	0.1
Aperture width	L	1m
Concentration ratio	C	1.18
Absorber width	s	0.85
CPC height	$\bar{h}$	0.17m

Appendix C: Yearly Performance of Collectors

Table 8: Yearly Performance of Collectors for Nicosia

Collector	Useful solar energy gain [10^6kJ]	Required auxiliary energy [10^6kJ]	Collector efficiency [-]
CPC	6.29	1.46	44.8
Flat Plate Collector	5.11	2.09	36.4

Table 9: Yearly Performance of Collectors for London

Collector	Useful solar energy gain [10^6kJ]	Required auxiliary energy [10^6kJ]	Collector efficiency [-]
CPC	2.18	5.57	31.8%
Flat Plate Collector	1.45	6.20	21.1%